

VYSOKÉ UČENÍ TECHNICKÉ V BRNĚ
BRNO UNIVERSITY OF TECHNOLOGY

FAKULTA ELEKTROTECHNIKY A KOMUNIKAČNÍCH TECHNOLOGIÍ
ÚSTAV RADIOELEKTRONIKY

FACULTY OF ELECTRICAL ENGINEERING AND COMMUNICATION
INSTITUTE OF RADIO ELECTRONICS

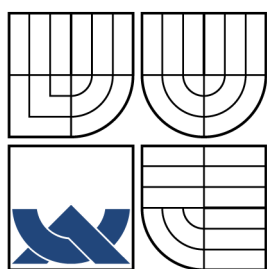
MODELOVÁNÍ KMITOČTOVĚ SELEKTIVNÍCH POVRCHŮ
V PROGRAMU COMSOL MULTIPHYSICS

DIPLOMOVÁ PRÁCE
MASTER'S THESIS

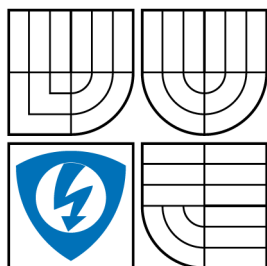
AUTOR PRÁCE
AUTHOR

TOMÁŠ HÖHN

BRNO 2008



VYSOKÉ UČENÍ TECHNICKÉ V BRNĚ
BRNO UNIVERSITY OF TECHNOLOGY



FAKULTA ELEKTROTECHNIKY
A KOMUNIKAČNÍCH TECHNOLOGIÍ
ÚSTAV RADIOELEKTRONIKY



FACULTY OF ELECTRICAL ENGINEERING AND
COMMUNICATION
INSTITUTE OF RADIO ELECTRONICS

MODELOVÁNÍ KMITOČTOVĚ SELEKTIVNÍCH POVRCHŮ V PROGRAMU COMSOL MULTIPHYSICS MODELING FREQUENCY SELECTIVE SURFACES IN COMSOL MULTIPHYSICS

DIPLOMOVÁ PRÁCE
MASTER'S THESIS

AUTOR PRÁCE
AUTHOR

Vedoucí práce
Supervisor

TOMÁŠ HÖHN

Prof. Dr. Ing. Zbyněk Raida

BRNO 2008

ZDE VLOŽIT LIST ZADÁNÍ

Z důvodu správného číslování stránek

ZDE VLOŽIT PRVNÍ LIST LICENČNÍ
SMOUVY

Z důvodu správného číslování stránek

ZDE VLOŽIT DRUHÝ LIST LICENČNÍ
SMOUVY

Z důvodu správného číslování stránek

ABSTRAKT

Metoda konečných prvků implementovaná v programu COMSOL Multiphysics je využívána k analýze tzv. free-standing kmitočtově selektivních povrchů ve 3D. Tyto modely jsou následně doplněny o periodické okrajové podmínky. Dále jsou free-standing povrchy doplněny o vrstvy dielektrika a je zkoumán jejich vliv na modul činitele odrazu. V analytické části jsou vyhodnoceny vlivy počtu elementů diskretizační mřížky na přesnost výsledku a délku výpočtů. Výsledky jsou srovnávány vzhledem k výsledkům uvedeným v literatuře [5]. V závěrečné části práce je vysvětlen postup při generování m-file pro obdélníkový element a použití globálního optimalizačního algoritmu PSO, který automaticky upravuje rozměry vodivého motivu tak, aby bylo dosaženo průběhu modulu činitele odrazu podle požadovaného průběhu.

KLÍČOVÁ SLOVA

Frekvenčně selektivní povrchy, COMSOL Multiphysics, periodické okrajové podmínky, Particle Swarm Optimization, Free-standing povrchy, COMSOL Script

ABSTRACT

Finite Element Method (FEM) implemented in COMSOL Multiphysics is used to analyze free-standing frequency selective surfaces (FSS) in a 3-dimensional (3D) space. Practical procedures for using periodic boundary conditions were developed and tested. A case study concerning mesh grid density (number of elements) vs. results' accuracy in a tight relationship with the calculation time needed was worked out. Outcomes were compared with results published in [5]. The procedure how to generate the m-file for a middle placed rectangular patch is described in the last part of the thesis. Also, PSO is used to adjust element's dimensions to shape the module of reflection coefficient so it approaches the shape of the objective function.

KEYWORDS

Frequency Selective Surfaces, Finite Element Method, COMSOL Multiphysics, Periodic Boundary Conditions, Particle Swarm Optimization, Free-standing surface, COMSOL Script

HÖHN T. *Modelování kmitočtově selektivních povrchů v programu COMSOL Multiphysics*. Brno: Vysoké učení technické v Brně. Ústav radioelektroniky, 2008. Počet stran s. 60. Počet stran příloh s. 4. Diplomová práce. Vedoucí práce byl Prof. Dr. Ing. Zbyněk Raida.

PROHLÁŠENÍ

Prohlašuji, že svou diplomovou práci na téma „Modelování kmitočtově selektivních povrchů v programu COMSOL Multiphysics“ jsem vypracoval samostatně pod vedením vedoucího diplomové práce a s použitím odborné literatury a dalších informačních zdrojů, které jsou všechny citovány v práci a uvedeny v seznamu literatury na konci práce.

Jako autor uvedené diplomové práce dále prohlašuji, že v souvislosti s vytvořením této diplomové práce jsem neporušil autorská práva třetích osob, zejména jsem nezasáhl nedovoleným způsobem do cizích autorských práv osobnostních a jsem si plně vědom následků porušení ustanovení § 11 a následujících autorského zákona č. 121/2000 Sb., včetně možných trestněprávních důsledků vyplývajících z ustanovení § 152 trestního zákona č. 140/1961 Sb.

V Brně dne

.....
(podpis autora)

PODĚKOVÁNÍ

Děkuji vedoucímu diplomové práce Prof. Dr. Ing. Zbyňku Raidovi za účinnou metodickou, pedagogickou a odbornou pomoc a další cenné rady při zpracování mé diplomové práce.

V Brně dne

.....
(podpis autora)

CONTENTS

1	Introduction	13
2	Finite Element Method	15
2.1	Structure Discretization	15
2.2	Assembly of Matrices for Isolated Finite Elements	16
2.3	Assembly of a Joining Matrix	16
2.4	Unite of Isolated Elements	17
2.5	Boundary Conditions Definition	17
2.6	Matrix Problem Solution	18
3	Frequency Selective Surface Analysis	19
3.1	In-Plane Waves Application Mode	19
3.2	Vector Elements and Scalar Variables	19
3.3	Boundary Conditions	20
3.3.1	Perfect Magnetic Conductor	20
3.3.2	Electric Field	20
3.3.3	Perfect Electric Conductor	21
3.3.4	Scattering Boundary Condition	21
3.3.5	Continuity	21
3.3.6	Port	22
4	Frequency Selective Surface Analysis with Periodic Boundary Conditions	23
4.1	1 Dimensional FSS Without PBC	23
4.2	1 Dimensional FSS with Applied Periodic Boundary Conditions	25
5	Free-standing FSS AnylYSIS in 3D	28
5.1	Introduction	28
5.2	Model Description	28
5.3	Model Navigator	29
5.4	Options and Settings	30
5.5	Geometry Modeling	30
5.6	Boundary Settings	31
5.7	Mesh Generation	31
5.8	Computing the Solution	32
5.9	Postprocessing and Visualization	32
5.10	H-Polarization Model Modification	33
5.10.1	Equivalent Feeding Modes	34
5.11	Adding Periodic Boundary Conditions	34

6	Settings Case Study	36
6.1	A Comparison of Results Obtained with and without PBC	36
6.2	Feeding Boundary Position Analysis	37
7	Occupied Elements	40
8	Real Periodic Structures	43
8.1	Model of a Real Periodic Structure	43
8.2	Dielectric Thickness	44
8.3	Results Comparison With Theory	44
8.4	Circular Ring Element Analysis	46
9	Global Optimization Algorithm	48
9.1	Generating m-files	48
9.2	Particle Swarm Optimization	49
9.2.1	Code for the PSO	50
9.3	Results	51
10	Conclusion	53
	Bibliography	54
	Symbols and Definitions	55
	Appendix	56
A	M-file of the model	57
B	PSO code	59

LIST OF FIGURES

1.1	Frequency Selective Surface	13
2.1	2D finite element net template	15
2.2	2 Dimensional finite element for a linear approximation	16
4.1	2D In-Plane Waves model settings	23
4.2	1 Dimensional slot type FSS, TE	24
4.3	Reflection coefficient curve for a 1 Dimensional slot type FSS	25
4.4	1 Dimensional slot type FSS with PBC, TE	25
4.5	Reflection coefficient curve for the 1 Dimensional slot type FSS with applied PBC	26
5.1	A rectangular free-standing FSS	28
5.2	The E-polarization Port settings	32
5.3	The module of the reflection coefficient for the E-polarization	33
5.4	The module of the reflection coefficient for the H-polarization	34
6.1	The module of the reflection coefficient for the E-polarization with different mesh densities and PBC used	38
6.2	The feeding boundary position for the E-polarization (works for the H-polarization as well)	39
7.1	Rectangular patches placed in the corners and crossing the borders of the air box	40
7.2	The final occupied structure with conductive patches placed in corners	41
7.3	The E-polarization reflection curves for the redrawn structure	42
8.1	A model of a real structure	44
8.2	E-polarization reflection curves for variable dielectric thicknesses d with $\epsilon_r = 4$	45
8.3	A circular ring element model	46
8.4	The E-polarization reflection curve for a circular ring element	47
8.5	The transmission loss curve for a circular ring element published in [4]	47
9.1	Resulting reflection coefficient curves after several PSO runs	51

LIST OF TABLES

2.1	Joining matrix	17
5.1	The Application Scalar Variables Settings	30
5.2	FSS and air box dimensions	31
5.3	The rectangular patch boundary settings using PBC	31
5.4	Boundary modifications for the H-polarization	33
5.5	Source and destination vertices numbers used for PBC	35
6.1	The feeding edge position, mesh density and a calculation time for the E-polarization without using PBC	36
6.2	The feeding edge position, mesh density and a calculation time for the E-polarization with PBC	37
6.3	The feeding edge position, mesh density and a calculation time for the H-polarization without using PBC	37
6.4	The feeding edge position, mesh density and a calculation time for the H-polarization without using PBC	37
7.1	Source and destination vertices numbers used for the redrawn structure with PBC	41
8.1	A solution time table with expected new values for various thicknesses of dielectrics	46
9.1	PSO results	51

1 INTRODUCTION

Frequency Selective Surface (FSS)s are periodic structures consisting of electrically conducting elements (can be of various shapes, e.g. rectangular patches, dipoles, crosses, etc.) placed on the dielectric substrate. Another available arrangement consists of magnetic elements (slots on the conducting substrate). An incident electromagnetic wave induces electric currents on the elements. If a secondary electromagnetic wave radiated by the induced currents interferes in phase with the incident wave, the selective surface acts as a reflector. If the interfering waves meet with an opposite phase, reflected wave is zero and a selective surface behaves as a free space [1], [2]. FSSs can be used as frequency dependent reflectors (reflecting just at certain frequencies), as band-pass radomes used to reduce the radar cross section of antennas outside their operating band (waves at operating frequencies are propagating through) and for other, mainly military, purposes [1], [2]. An ideal selective surface is infinitely

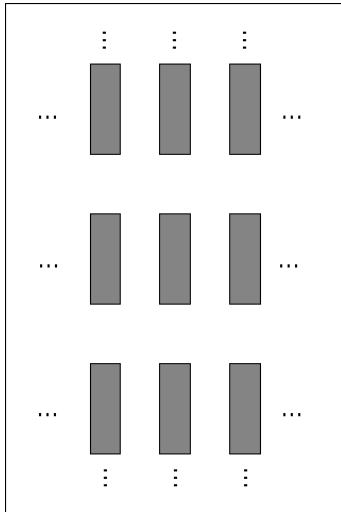


Fig. 1.1: Frequency Selective Surface.

large plane, what (not at first sight) simplifies numerical analysis of such a structure. Nowadays, two approaches are used:

1. **Method of Moments in Spectral Domain.** A spatial spectra are calculated from unknown current distributions on conducting elements (distributions are the same at all elements). Since elements are placed periodically, the spectra are discrete and unknowns then take a form of coefficients, which values are acquired by solving a matrix problem. By substituting them, the current spatial distribution is found [1].
2. **Periodic Boundary Conditions.** Just one element is numerically analysed. If such an element is enclosed with edges, which mirror the element to infinity, one infinitely large periodic structure is obtained. Used edges for such special purpose are called Periodic Boundary Conditions (PBC), [1].

The first part of the project is dedicated to principals of the Finite Element Method (FEM), particularly to a matrix problem leading to the method's solution.

Moreover, specific properties of a COMSOL In-Plane Waves Module used to all numerical analysis are described. The theoretical part of this Diploma thesis deals with a description and problematics of boundary conditions and their use in COMSOL Multiphysics.

Non reflecting edges and periodic boundary conditions functionality is verified in the practical part.

2 FINITE ELEMENT METHOD

FEM is a general numerical method used to solve partial differential equations. Since Maxwell equations can be transcribed to this form, the finite element method can be exploited to solve them. The finite element method consists of following steps.

2.1 Structure Discretization

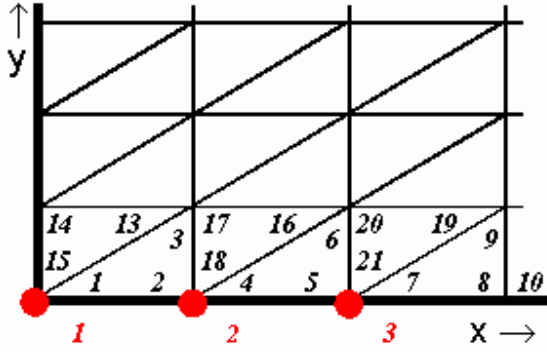


Fig. 2.1: 2D finite element net template. blue numbers: local nodes. red numbers: global nodes.

A discretization of the structure done by its division to a finite number of geometrical shapes (see Fig. 2.1) has to be made preceding the own numerical analysis. The best discretization method offering a compromise between the accuracy and the calculation time is a Delaunay's triangulisation, permitting structure division into mutually non overlapping triangles (triangles are adjacent). Delaunay's travelling front triangulisation, Bowyer-Watson or Green-Gibson method are the most used meshing approaches. Last two methods provide an adaptive discretization (a smooth transition from a coarse to a finer mesh grid) [1]. The main motion of the discretization (meshing) is a necessity of doing an electromagnetic's field formal approximation over a satisfactory amount of discretization elements. A term formal denotes, that the field is computed on the basis of unknown node values (triangle vertices) using basis functions (may be linear, quadratic or cubic), where the basis function over one triangle is defined as a function with unit value at one vertex and zero value at remaining vertices. Formal approximation results form an input into the original wave equation (this procedure is mathematically described in section 2.6), which for TM modes in a rectangular metallic waveguide look as [1]:

$$\frac{\partial^2 e}{\partial x^2} + \frac{\partial^2 e}{\partial y^2} + (k_0^2 - \beta^2) e = R(x, y) \quad (2.1)$$

A phase constant β denotes a phase change per length unit, $k_0^2 = \omega^2 \mu_0 \epsilon_0$ is a wave number of the propagating wave and the right side $R(x, y)$ is a so called residual function, which minimisation is done by weighting itself with basis functions.

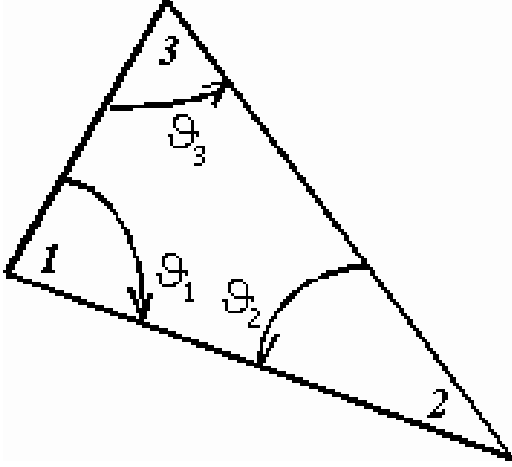


Fig. 2.2: 2 Dimensional finite element for a linear approximation.

2.2 Assembly of Matrices for Isolated Finite Elements

Properties of all discretization elements have to be known before trying to proceed the formal approximation of the electromagnetic field. Matrix transcripts for normed mesh elements are used to provide easier and faster calculations, e.g. for a triangle (see Fig. 2.2) and a linear approximation holds [1]:

$$\mathbf{Q}_1 = \frac{1}{2} \begin{bmatrix} 0 & 0 & 0 \\ 0 & +1 & -1 \\ 0 & -1 & +1 \end{bmatrix} \quad \mathbf{Q}_2 = \frac{1}{2} \begin{bmatrix} +1 & 0 & -1 \\ 0 & 0 & 0 \\ -1 & 0 & +1 \end{bmatrix} \quad \mathbf{Q}_3 = \frac{1}{2} \begin{bmatrix} +1 & -1 & 0 \\ -1 & +1 & 0 \\ 0 & 0 & 0 \end{bmatrix} \quad (2.2)$$

Matrices above are used to calculate matrices of coefficients for every e isolated finite element [1]

$$\mathbf{S}^{(e)} = \sum_1^3 \mathbf{Q}_n \cot g v_n^{(e)} \quad (2.3)$$

and

$$\mathbf{T}^{(e)} = \frac{\mathbf{A}^{(e)}}{12} \begin{bmatrix} 2 & 1 & 1 \\ 1 & 2 & 1 \\ 1 & 1 & 2 \end{bmatrix}, \quad (2.4)$$

where $A^{(e)}$ is an area of the triangle.

2.3 Assembly of a Joining Matrix

According to an arbitrary chosen system, which has to be followed throughout the whole numbering procedure, local nodes are numbered (see Fig. 2.1) counterclockwise starting before the 90° angle. Global matrices of coefficients are assembled

from well known matrices of coefficients for each discretization element [1]

$$\mathbf{S} = \begin{bmatrix} \mathbf{S}^{(1)} & 0 & 0 & 0 \\ 0 & \mathbf{S}^{(2)} & 0 & 0 \\ 0 & 0 & \mathbf{S}^{(3)} & 0 \\ 0 & 0 & 0 & \dots \end{bmatrix} \quad \mathbf{T} = \begin{bmatrix} \mathbf{T}^{(1)} & 0 & 0 & 0 \\ 0 & \mathbf{T}^{(2)} & 0 & 0 \\ 0 & 0 & \mathbf{T}^{(3)} & 0 \\ 0 & 0 & 0 & \dots \end{bmatrix}, \quad (2.5)$$

where zeros denotes zero matrices with dimensions 3x3 (matrix dimensions must be maintained to allow a correct matrix multiplication).

2.4 Unite of Isolated Elements

An aim of this procedure is to describe relations between local and global nodes. First, a so called unite (joining) matrix \mathbf{C} has to be set up. An illustrative example below shows a content of the joining matrix \mathbf{C} .

Finally, joining of isolated elements using the equation below takes a place [1]:

$$\mathbf{S}_C = \mathbf{C}^T \mathbf{S} \mathbf{C}, \quad \mathbf{T}_C = \mathbf{C}^T \mathbf{T} \mathbf{C} \quad (2.6)$$

Tab. 2.1: Joining matrix. Rows relate to local nodes, columns then to global nodes. Values "1" sign the local node's membership to a global node. It is clear from a comparison shown in Fig. 2.1, where global nodes counterclockwise numbering was used, that local nodes 1 and 15 are joined (pertain) to the global node 1 [1].

	1	2	3	
1	1	0	0	= \mathbf{C}
2	0	1	0	
3	0	0	0	
4	0	1	0	
5	0	0	1	
6	0	0	0	
7	0	0	1	
15	1	0	0	
18	0	1	0	
21	0	0	1	

2.5 Boundary Conditions Definition

A boundary conditions definition varies from one application to another. Basics can be most easily described on a longitudinally homogeneous rectangular waveguide. TM modes are expressly determined by a distribution of an electric field longitudinal component E_Z . This component must be zero on all conducting surfaces of the waveguide (fulfils Dirichlet's condition). Practically, we deal with this condition by slightly modifying the joining matrix \mathbf{C} , so all rows and columns referring to global nodes are left out.

2.6 Matrix Problem Solution

A solution of a matrix problem is expressed with the equation [1]

$$\mathbf{SE} + k^2\mathbf{TE} = \mathbf{0}. \quad (2.7)$$

The numerical analysis result of this equation is a vector of eigenvalues k^2 and a matrix of eigenvectors \mathbf{E} . Quadrates of eigenvalues k^2 depict critical frequencies of individual modes and each matrix \mathbf{E} contains electric field intensity values on each node. Those intensity values are then substituted into the formal approximation which represents the longitudinal intensity component over each discretization element.

In the next chapter, an analysis of an electromagnetic structure using the finite element method in COMSOL Multiphysics will be exposed.

3 FREQUENCY SELECTIVE SURFACE ANALYSIS

3.1 In-Plane Waves Application Mode

Since each application mode is defined by a differential equation, an appropriate application mode has to be chosen preceding drawing the geometry and its analysis.

The In-Plane Waves Module is intended for structures with no variation in z axis and wave propagating only in (x, y) plane. This application model offers solutions for following field type distributions:

- TE waves
- TM waves
- TEM waves (*hybrid mode waves*). TEM wave is defined by a TE and TM waves superposition. Moreover, the incoming wave can be defined as an elliptic or a circular wave. Neither of two definitions was used in this Diploma thesis (the incident field is always defined as a plane wave).

It can be stated for an electromagnetic field propagating in modelled (x, y) plane, that only one non zero component for TE wave is presented (the one in z axis) and that the magnetic field is suppressed to propagate only in the modelled plane. Harmonic electric and magnetic field vectors can be then defined using equations [3]

$$\mathbf{E}(x, y, t) = E_z(x, y, t) = E_z(x, y) \mathbf{e}_z e^{j\omega t} \quad (3.1)$$

$$\mathbf{H}(x, y, t) = H_x(x, y, t) \mathbf{e}_x + H_y(x, y, t) \mathbf{e}_y = (H_x(x, y) \mathbf{e}_x + H_y(x, y) \mathbf{e}_y) e^{j\omega t} \quad (3.2)$$

Vectors \mathbf{E} and \mathbf{H} defines the electric and the magnetic field, where individual vector components are distinguished using a subscript. Variable ω is as commonly used to mark an angular frequency.

A more detailed theoretical and mathematical analysis concerning TE, TM and hybrid TEM waves propagation is also mentioned in [3]. Since the one is used for the FSS problem analysis (in 2D), a deeper application model knowledge is advised.

3.2 Vector Elements and Scalar Variables

According to the COMSOL documentation, a limited input scalar variables amount can be used under different application modes. Those are for a planar wave propagation $\mu_0, \varepsilon_0, \nu_0, \lambda_0$, where first two quantities refer to permeability and permittivity in vacuum. If we want to solve a field distribution in a settled state (*harmonic problem*), frequency ν_0 or a vacuum wavelength λ_0 has to be defined. This listing ends here for our model, though the listing for a 3D application mode is widened.

3.3 Boundary Conditions

Physical properties (again mostly the permittivity and the permeability) need to be attached to model layers, after these have been designed (using COMSOL designing tools or imported from a supported CAD program). A properties edit tool can be found under *Subdomain Settings* from the *Physics* menu. A total parameters amount quite varies - from a possibility of using predefined materials up to a tensor character definition.

The next in the row is boundary settings on boundaries and edges (through *Boundary Conditions* from the *Physics* menu. Their choice is driven by needs laid on a model functionality. Using them, we tell the program how we wish the field to look like on the boundary or in the near neighbourhood. The In-Plane Waves Module allows the user to choose (with restrictions) from thirteen different types of boundary conditions. Their description follows, since the right way of using them is a key to a modeling of FSS.

3.3.1 Perfect Magnetic Conductor

We begin with Perfect Magnetic Conductor (PMC), on which surface field fits the condition [3]

$$\mathbf{n} \times \mathbf{H} = \mathbf{0}, \quad (3.3)$$

where \mathbf{n} denotes the normal vector.

Choosing this condition makes the program to force a zero value to the tangential of magnetic field on the boundary.

PMC can be as well applied on interior boundaries if the propagating wave is TM.

3.3.2 Electric Field

Boundary condition (*Electric Field*) is defined by the equation [3]

$$\mathbf{n} \times \mathbf{E} = \mathbf{n} \times \mathbf{E}_0, \quad (3.4)$$

where the \mathbf{E}_0 vector value refers to (by an user) set electric intensity value on a boundary.

This condition is with advantage used to set up arbitrary electric intensity values on the boundary. In addition to that, an incident field type (circle, elliptic or plane) can be chosen. We are completely allowed to exploit this phenomenon on interior boundaries only under harmonic analysis for TE modes.

3.3.3 Perfect Electric Conductor

Perfect Electric Conductor (PEC) is used in cases, when the tangential of an electric field intensity on the boundary or the near adjacent area wants to be forced to a zero value [3].

$$\mathbf{n} \times \mathbf{E} = \mathbf{0}. \quad (3.5)$$

In analogy with PMC, also PEC can be exploited for interior boundaries.

3.3.4 Scattering Boundary Condition

Scattering boundary condition introduces many new useful options to a finite element method solution problem. Choosing and setting a boundary to be of Scattering boundary type causes an incident field to propagate through the boundary without any insertion loss or reflections. Such a boundary keeps those properties for both the incident and the reflected field (reflected from objects placed behind the Scattering boundary, not from the boundary itself). Also, those special properties work on the same basis for cylindrical and plane incident waves, which intensities at the certain point can be determined as [3]

$$E = E_{SC}e^{-jk(\mathbf{n} \cdot \mathbf{r})} + E_0e^{-jk(\mathbf{k} \cdot \mathbf{r})} \quad \text{for a plane wave} \quad (3.6)$$

$$E = E_{SC} \frac{e^{-jk(\mathbf{n} \cdot \mathbf{r})}}{\sqrt{r}} + E_0e^{-jk(\mathbf{k} \cdot \mathbf{r})} \quad \text{for a cylindrical wave}, \quad (3.7)$$

which input variables are the normal vector \mathbf{n} , a position vector \mathbf{r} , a scattered wave electric intensity value E_{SC} and an electric intensity value created by an incident wave propagating from a direction described by a wave vector \mathbf{k} .

Scattering boundary conditions can be in suitable occasions replaced with Perfectly Matched Layers (PML). However, controlling the wave's behaviour is not a trivial task then. Even in the simplest cases the layer thickness has to be adjusted to the wavelength of a propagating wave. Moreover, one needs to keep an eye on the PML functionality and effectivity since rather big computing errors might occur in some situations. Also, PML does not belong to the boundary conditions set. Practically, PML is an adding domain, which absorbs fields without any reflections. We introduce PML to our design in cases we know a wave number of the incident field (wave).

3.3.5 Continuity

Fields modeling not rarely requires field continuity on the both sides of the edge (e. g. interface between the two dielectrics). To do so, a Continuity is presented. In terms of physics, electric and magnetic field tangential components are forced to be continuous on the both sides of the edge. Finally, a mathematical formulation [3]

$$\mathbf{n} \times (\mathbf{H}_1 - \mathbf{H}_2) = \mathbf{0} \quad \mathbf{n} \times (\mathbf{E}_1 - \mathbf{E}_2) = \mathbf{0}. \quad (3.8)$$

Subscripts 1 and 2 denotes the electric and the magnetic field on interfaces 1 and 2.

We encounter use of the continuity mostly for measuring edges inside the structure or on a transition between two subdomains representing the same material. One like this does not influence the field forming and propagating inside the design.

3.3.6 Port

The last boundary condition type with most useful options is called Port. We find its use to feed waveguides or other structures. Notice, that feeding can be done also using other boundary conditions (e.g. by setting up initial values for the Electric Field or by choosing the edge to be of the Scattering Boundary with its initial field value), but only Port allows parameter measurements without manually specified formulas. All variables appearing in these formulas have to be solved by modeling a field distribution within the structure beforehand.

S-parameters Calculated from a Field Distribution

S-parameter calculations using a Port boundary condition can be solved based on two different approaches. The first approach is to perform an eigenmode analysis and find *Fundamental Modes* on the ports. Fundamental mode values for port 1 and 2 and modeling in 2D are represented by vectors $\mathbf{E}_1, \mathbf{E}_2, \mathbf{E}_3$ (or by matrices in 3D). Further, fields (vectors or matrices) have to be normalized with respect to the integral of the power flow across each port cross section. Finally, \mathbf{E}_C consisting of an excitation plus the reflected field from the edge (b.c. port) is calculated. The s_{11} is given by [3]

$$s_{11} = \frac{\int_{port\ 1} ((\mathbf{E}_C - \mathbf{E}_1) \cdot \mathbf{E}_1^*) dA_1}{\int_{port\ 1} (\mathbf{E}_1 \cdot \mathbf{E}_1^*) dA_1} \quad (3.9)$$

S-parameters in Terms of Power Flow

The second option is to calculate s-parameters from the power flow through the port. This approach does not allow to determine the s-parameters phase component. Since we do not use this option in 2D, further properties description will stay left untouched. The formula just for the comparison with the eigenmode analysis approach follows [3]

$$s_{11} = \sqrt{\frac{P_{r1}}{P_{i1}}}, \quad (3.10)$$

where P_{i1} denotes a power incident on port 1 and P_{r1} represents a power reflected from port 1.

4 FREQUENCY SELECTIVE SURFACE ANALYSIS WITH PERIODIC BOUNDARY CONDITIONS

The first step while proving boundary conditions functionality (PBC are not involved yet) is to design and analyse a simple structure. Scattering boundary conditions will be tested and discussed in this chapter.

Each analysis is highly dependent on a used model choice (a bad model leads to bad results). Also, each model is described by its own (from other varying) differential equation.

For a planar wave propagation, we need to choose (from the COMSOL main menu) modeling in $2D$, then click on *TE Waves* in the *RF* folder and select *Harmonic propagation*. Element type shall remain on the initial value *Lagrange-Quadratic* (Fig. 4.1). The next step is to escape out of an awkward situation, when a just

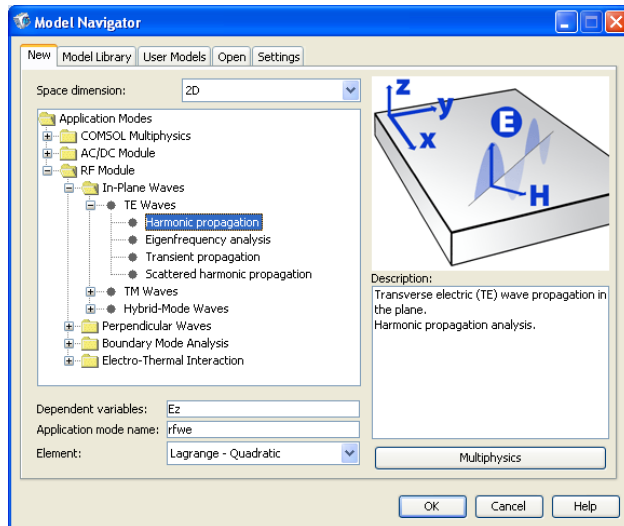


Fig. 4.1: 2D In-Plane Waves model settings.

one shape is known and properties of the infinitely large plane made of such shapes want to be find out. It is clearly understandable that we will not try to draw the whole plane, but an other elegant solution has to be employed. The solution is the application of PBC.

4.1 1 Dimensional FSS Without PBC

First, a simple structure without using PBC will be analyzed since this approach can lead to sufficient results in some cases. In our case, the structure will be a *slot type* FSS element. We can imagine the whole arrangement (see Fig. 4.2) as infinitely long metal stripes (rising up from the paper plane) of the 0.4 m height, 0.02 m width and 0.4 m distance separating two neighbouring stripes. The feeding (source) edge is placed 0.5 m on the left, destination edge then 0.5 m on the right.

Many times mentioned In-Plane Waves Module set up according to Fig. 4.1 will be employed during the analysis. Comments on used boundary conditions have to

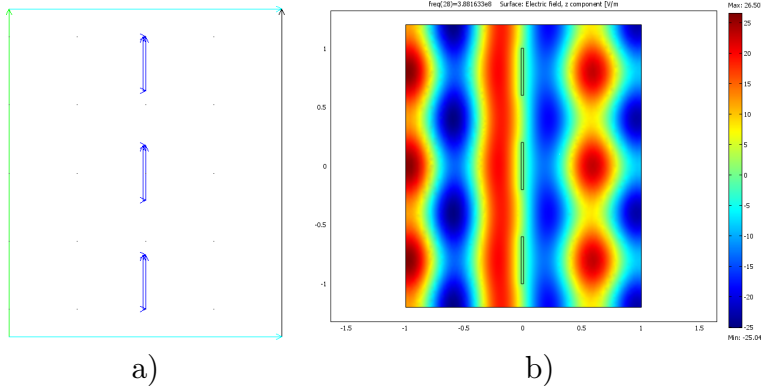


Fig. 4.2: 1 Dimensional slot type FSS, TE: a) boundary conditions; green – Port, blue – PEC, azure – PMC, black – Scattering Boundary Condition (Plane wave, Electric field, $E_{0z} = 0 \text{ Vm}^{-1}$), b) field distribution at frequency 388 MHz (first null).

be made. The left (green) edge plays the feeding (source) edge role. The feeding is done using Port, but on appropriate places its unique number (in our case "1"), the feeding power (1 W) radiated out of the port and the desired electric intensity value $E_{0z} = 0 \text{ Vm}^{-1}$ have to be specified.

However, using ports is a two face issue. The advantage might be, that a reflection coefficient is automatically calculated (no need to define complicated analytical equations) once at least one feeding port is defined in the structure. Definite disadvantage due to wave reflections is a slightly lower solution accuracy if the port was placed [3].

Worth mentioning are by azure color highlighted edges (working as PMC). Since we want our structure driven by a plane wave, Scattering boundary conditions can not be chosen. Their use would cause a part of the wave energy leaking through the top and the bottom edge. Therefore PMC to create an optimal feeding (looks like the feeding was done from an infinitely long wall) are employed.

Remaining, blue edges, signalling (just in this case) PEC and black (destination) edge working as Scattering boundary conditions do not bring any progress to modeling problematics and are not worth commenting.

This comment lack does no longer hold for a parametric analysis setup – made from menu *Solve, Solve Parameters*. We type **freq** into the *Name of Parameter* field and **linspace(300e6,460e6,50)** into the *List of Parameter Values* field. The **Linspace** function secures the solution calculation on fifty equidistantly placed frequencies in the range from 300 MHz to 460 MHz. Finally, the text **freq** has to be typed next to the field *nu_rfwe* in the scalar variables table.

Expectations of a resonance appearing at the frequency 375 MHz are fully right considering structure dimensions. This theoretical value can be compared with the s_{11} reflection coefficient curve (see Fig. 4.3). Since the reflection coefficient is defined on the whole structure, any from offered points shown in *Postprocessing, Domain Plot Parameters, Point, Point Selection* listbox can be used.

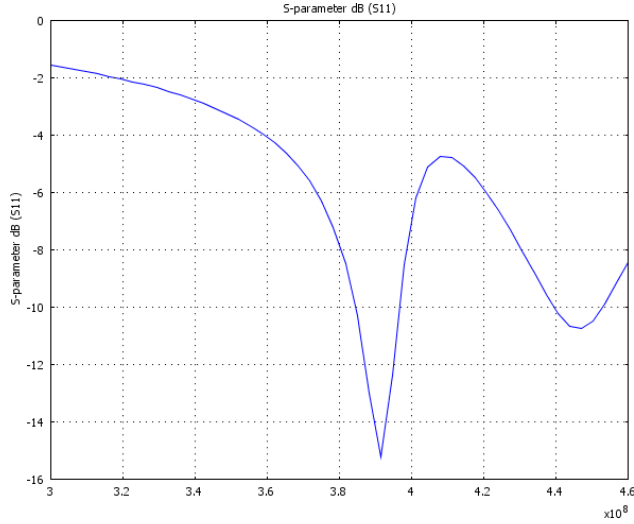


Fig. 4.3: Reflection coefficient curve for a 1 Dimensional slot type FSS.

4.2 1 Dimensional FSS with Applied Periodic Boundary Conditions

As stated earlier, the effective modeling can be achieved only if the analysis is executed on a just one single element. This can not be held out other way than using PBC. Fundamental for this operation is a structure shown in Fig. 4.4 top. The PBC setup is controlled from menu *Physics, Periodic Conditions, Periodic*

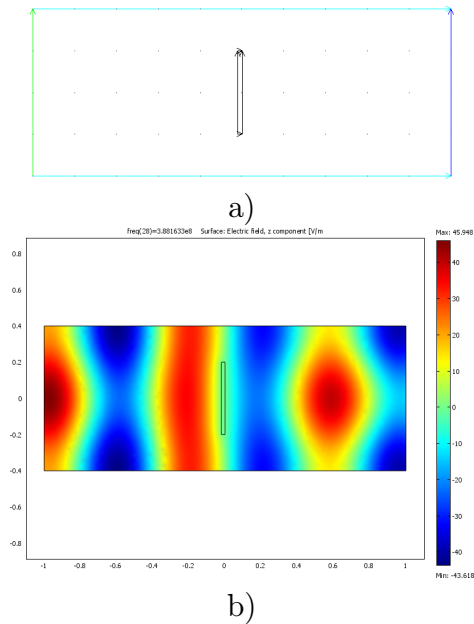


Fig. 4.4: 1 Dimensional slot type FSS with PBC, TE: a) boundary conditions; green – Port, black – PEC, azure – PMC, blue – Scattering Boundary Condition (Plane wave, Electric field, $E_{0z} = 0 \text{ Vm}^{-1}$), b) field distribution at frequency 388 MHz (first null).

Boundary Conditions. The opened window contains four tabs in total. Two for the edge definition (the source and destination) and two for definition of the source and destination vectors. The aim is to setup PBC so the structure seems to be infinitely long in the vertical direction. The top edge will be considered as the source edge.

In the *Source* tab a number corresponding to the top (azure) edge shall be chosen and text **Ez** should be typed into the *Expression* field. Text **pconstr1** in the field *Constraint name* is generated automatically, but can be replaced with an arbitrary text.

Not ment to be changed is the parameter name in the **Expression** field. This parameter is strictly dependent on the used model and is always stated in the window intended to the model selection (see Fig. 4.1) – we find it next to the *Dependent variables* field.

After switching to the *Destination* tab, we choose a number corresponding to azure edge and tick on the checkbox next to the number (alternatively *Use selected boundaries as destination* can be ticked). Finally, we type text **Ez** into the *Expression* field.

Source and destination edges are now defined. Also, each abscissa is defined by two points (vertices). Reading in the *Source Vertices* field has to be filled in so *Source vertices* list contains left and right vertices numbers moved from the section on the left. Vertices numbers have to be selected in a fixed order. Edge directions (the source and the destination) can be chosen arbitrarily (from the left to the right in our case), but always in the same direction throughout the one element.

Confirm the settings by clicking on *OK* button, after you have defined vertices numbers in *Destination Vertices* tab (in order left – bottom, right – bottom).

The parametric analysis setup is the same as in the 1 Dimensional FSS analysis case without PBC. Its result is a reflection coefficient curve on the input (see Fig. 4.5), which has no dissimilarities comparing to the curve obtained during the analysis without using PBC. Both draw curves were obtained with meshing

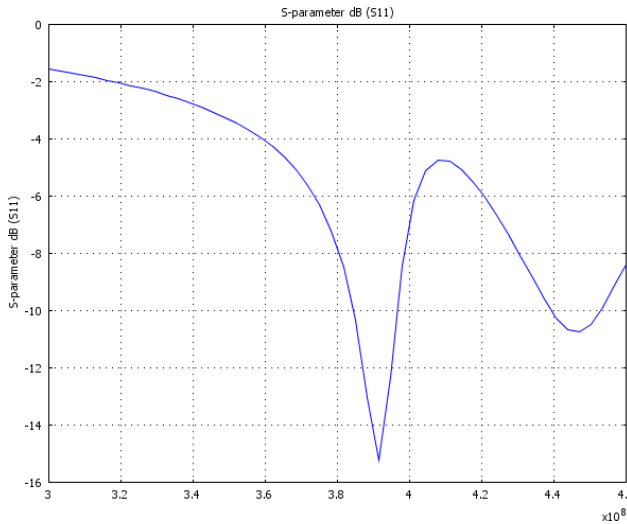


Fig. 4.5: Reflection coefficient curve for the 1 Dimensional slot type FSS with applied PBC.

set to *Normal*. Increasing the mesh density does not lead to any markable changes in the result's accuracy. So the meshing mode *Normal* is satisfying and it is completely useless to employ meshing grids with super high density which in consequence lead to a long result time.

5 FREE-STANDING FSS ANYLYSIS IN 3D

So far, this thesis has been dealing with 2D objects (planes of various shapes) and their periodicity in one dimension¹. To be able to move on and analyze structures in a 3D with periodicity in two dimensions (plane), the In-Plane Waves Module needs to be leaved and a 3D Electromagnetic Waves module will be used instead.

First functionality tests will be worked out on a so called free-standing surface made of a rectangular shape. These results will be compared to results published in [5] afterwards.

5.1 Introduction

Since all models showed throughout the thesis are somewhat derived and pulled up from demo and teaching models published at Comsol international websites or distributed with the installation package, the model documentation format is maintained according to those materials.

5.2 Model Description

The goal is to design and analyse a structure shown in Fig. 5.1 in a frequency range from 1 GHz to 50 GHz with a 1 GHz frequency step. A middle placed conductive

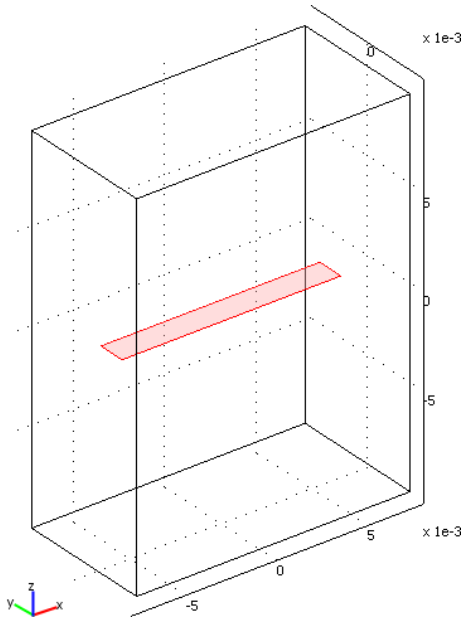


Fig. 5.1: A rectangular free-standing FSS.

patch, according to [2] belonging to a solid interior group, is surrounded by an

¹It is recommended that reader spots the difference between the two terms – the first is describing the space dimension of the designed structure and the latter is defining a number of dimensions, in which the structure will be extended to infinity.

imaginary air block helping us to set up a source of an incident radiation (the top boundary) and define gaps between single FSS elements forming the whole plane. The conductive element is considered to be a free-standing. The term free-standing well known from a FSS theory refers to a perfectly electrically conducting plane, which thickness is typically less than $\lambda/1000$ [2]. No dielectrics is presented either over or under the conductive patch. General solid interior group elements are assumed to have a first resonance when their largest length is approximately equal to $\lambda/2$. For example, for the biggest length $12 \cdot 10^{-3}$ m, the first resonance is expected around 12.5 GHz.

The incident plane wave, with E component directing in the x direction, propagates from the top boundary towards the conductive element, where some part of it is deflected and the rest continues its way until it reaches the bottom (ideally) non-reflecting boundary. Finally, side walls help the wave sustain its plane wave character and force it to stay within the block's boundaries. The back and the front wall are assumed to be PMC and the left and the right wall are assumed to be PEC.

The key factor of modeling is a distance between the feeding (source) edge and the conductive element. The optimal distance for an investigated frequency band 1 GHz-50 GHz is $\lambda/2$ at the frequency 15 GHz. Comparing to this optimal feeding edge position, moving the feeding edge closer to the patch causes incorrect results, whether moving it in the opposite direction leads just to increased amount of calculation time while the results are still correct. An appropriate analysis and a discussion on the feeding topic is given in Chapter 6.2.

If we flip through a literature dedicated to FSS, we come to a fact that characteristics of a single element are a function of the polarization and the angle of incidence. We can easily solve polarization issues. Unfortunately, we can not as easily deal with angle issues. Basically, there are two options available in COMSOL – neither leading to curves containing both the polarization and the angle of incidence dependencies at the same time.

The first option, 3D Scattered Waves Module originally intended to solve the reflected field scE offers a good scE accuracy and a little worse total field E solution accuracy. Also, the routine handling the angle of incidence can be easily implemented (without changing the shape of the geometry). What makes the module practically unusable is a fact, that Port availabilities do not work and one has to perform an eigenmode analysis in order to compute reflection coefficient values.

As follows from the previous discussion, the second – 3D Electromagnetic Waves module is the only handy module we end up to work with. The polarization is controlled using an appropriate Port settings, scE is computed while tolerating the error and reflection coefficient values are computed automatically. All with no control over the angle of incidence (the only way left is to manually change the structure's geometry for every angle of incidence).

5.3 Model Navigator

1. In the *Model Navigator*, select *3D* from the *Space dimension* list.
2. In the *RF Module* folder, select *Electromagnetic Waves* and *Harmonic propagation*.

3. Choose *Vector, Linear* from the *Element* list.
4. Click *OK*.

5.4 Options and Settings

1. From the *Physics* menu, choose *Scalar variables*.
2. In the *Application Scalar Variables* box, change two *Expressions* as stated in Tab. 5.1.
3. Click *OK*.

Tab. 5.1: The Application Scalar Variables Settings.

NAME	VALUE	DESCRIPTION
<i>nu_rfw</i>	<i>freq</i>	Variable name used to parametric analysis
<i>E0iz_rfw</i>	0	Incident electric field, <i>z</i> component

5.5 Geometry Modeling

As already mentioned in previous chapters, drawing the structure should be considered anything but a simple task. Although the object can look the same after taking different procedures, it seldom is the same. The whole act of manually typing in object dimensions does not cause the main damage. Most bugs, resulting in wrong curves and increases in a calculation time are caused by a misconception of using subdomains. Everytime two or more overlapping subdomains are encountered, a composite object consisting of them should be created. Note this step does not have to be proceeded immediately after domains have been drawn (since changes to once created composite objects are possible only in a limited extent, therefore it is wise keeping the original domains as long as possible to be able to change their dimensions), but has to be proceeded before the meshing procedure.

The drawing interface offers the *Embed* feature. Embedding is in COMSOL analysis mostly used to create conductive patterns (substitutes a term etching in technology) on a printed circuit board (e.g. patch antennas), but can be used to create face objects as well. The face object is a plane – not a subdomain, appears as an infinitely thin layer and is not meshed. Put a little bit more precisely, only its inner volume is not meshed (since there is not one). Their proper use helps to decrease a number of mesh points and rapidly speeds up calculations.

All dialog boxes for specifying the primitive objects are accessed from the *Draw* menu and *Specify Object*. The software generates the content of the Name column in the tables below automatically, so you do not have to enter them. Just check that you get the correct name for the objects that you create.

Begin by creating a work plane for the conductive stripe:

1. From the *Draw* menu, select *Work Plane Settings*.
2. In the Work Plane Settings dialog box, select the $x - y$ plane at z equal to 0. Click *OK*.

Tab. 5.2: FSS and air box dimensions.

NAME	WIDTH	HEIGHT	BASE	(X,Y)	DESCRIPTION
R1	$12 \cdot 10^{-3}$	$1.5 \cdot 10^{-3}$	Center	(0,0)	Conductive element
R2	$15 \cdot 10^{-3}$	$7.5 \cdot 10^{-3}$	Center	(0,0)	Air wall boundaries

3. Draw two rectangles with the properties according to Tab. 5.3.
4. Select the small rectangle, R1, and select *Embed* from the *Draw* menu.
5. From the *Draw* menu, select *Work Plane Settings*.
6. Select the (x,y) plane and set z equal to -0.01 . Click *OK*. This will change the location of the work plane in the z axis in the 3D geometry.
7. Select the big rectangle, R2, and select *Extrude* from the *Draw* menu.
8. In the *Extrude* dialog box, enter 0.02 in the *Distance* field, and select *Geom1* from the *Extrude geometry* list. Click *OK*.

5.6 Boundary Settings

1. From the *Physics* menu, open the *Boundary Settings* dialog box, select the *Interior boundaries* check box, and enter the settings according to the Tab. 5.3 (leave all remaining fields at their default values).
2. Click *OK*.

Tab. 5.3: The rectangular patch boundary settings using PBC.

BOUNDARY	3			
Boundary condition	Scattering boundary			
Wave type	Plane wave			
Incident field	Wave given by incident field			
BOUNDARY	1, 6, 7	2, 5	4	
Boundary condition	PEC	PMC	Port	

The port boundary condition settings should be set according to Fig. 5.2

5.7 Mesh Generation

Since the structure of the model is simple (no dielectrics and complicated shapes are presented), an interactive meshing procedure can be used.

1. Click the *Geom1* tab.
2. From the *Mesh* menu, choose *Interactive Meshing>Delete Mesh*.
3. From the *Mesh* menu, choose *Free Mesh Parameters*.
4. From the *Free Mesh Parameters* dialog box, select *Normal* in the *Predefined mesh sizes* list.
5. Click *Remesh*.
6. Click *OK*.

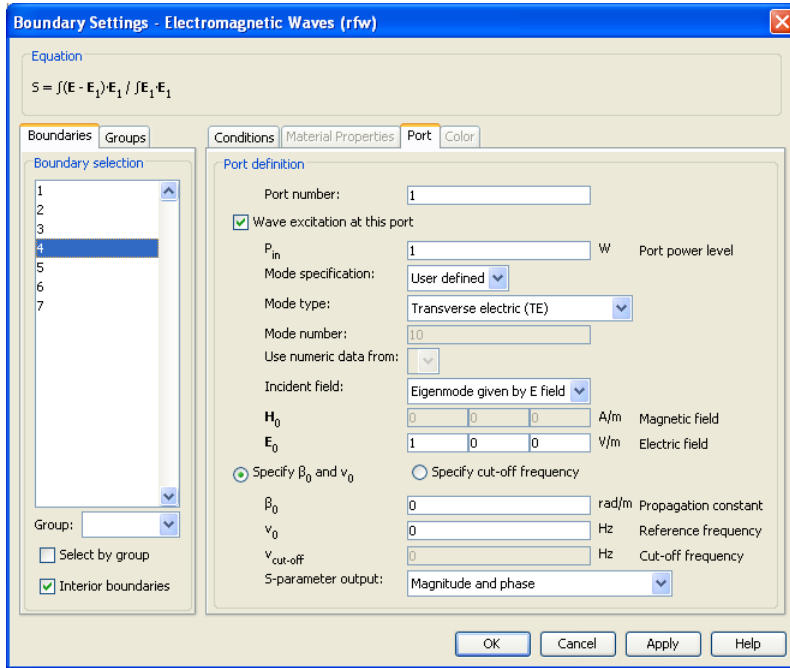


Fig. 5.2: The E-polarization Port settings.

5.8 Computing the Solution

1. Open the *Solver Parameters* dialog box from the *Solve* menu.
2. Select *Parametric* from the *Solver* list.
3. Type `freq` into the *Name of parameter* edit field and `linspace(1e9,50e9,50)` into the *List of parameter values* edit field.
4. Click *OK*.
5. Click on the *Solve* toolbar button.

5.9 Postprocessing and Visualization

1. Select *Domain Plot Parameters* from the *Postprocessing* menu.
2. Choose the *Point* tab, and select *S-parameter dB (S11)* from the *Predefined quantities* list.
3. Choose any number from the *Point selection* list (S-parameters are defined on the whole structure).
4. Click *OK*.

The result of previous operations is a module of the reflection coefficient shown in Fig. 5.3. The curve is plotted against the ideal solution obtained with [5] and together with curve obtained with PBC, which settings are described in Chapter 5.11. We can see, that the both curves obtained with COMSOL Multiphysics are shifted downwards in the frequency by approximately 2 GHz and its shape in a range from 24 GHz to 37 GHz is less than similar to the ideal curve. Anyway, both null positions are identical and the shape of the curves obtained with and without PBC are very close.

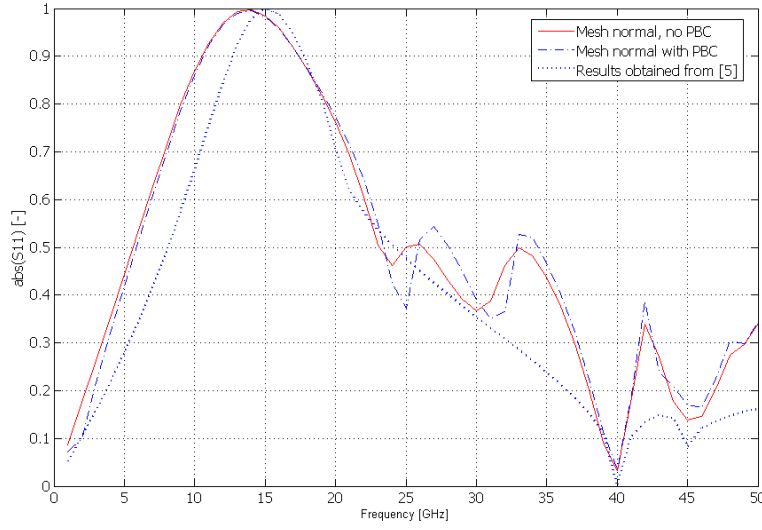


Fig. 5.3: The module of the reflection coefficient for the E-polarization.

5.10 H-Polarization Model Modification

Just minor model settings adjustments have to be taken to calculate reflection coefficient curves also for the H-polarization. To do so, the procedure from Chapter 5.3 to 5.9 should be followed, except the Chapter 5.6, where these steps need to be worked out:

1. Two pairs of the boundary settings have to be changed according to the Tab .5.4 (the remaining boundary settings stay the same as for the E-polarization settings).
2. In the *Port* boundary settings, *Electric field* component $E0x$ has to be set to zero and $E0y = 0 \text{ Vm}^{-1}$.

Tab. 5.4: Boundary modifications for the H-polarization.

BOUNDARY	2, 5	1, 7
Boundary condition	PEC	PMC

There are more nonsimilarities in the H-polarization case. A null at frequency 40 GHz is now shifted upwards for curves obtained with COMSOL and also, a null at 20 GHz is missing comparing to [5]. Since this fall is very sharp, one might argue whether the the code used in [5] to reach this curve is working properly. Again, curves obtained with and without using PBC are almost perfectly identical.

Despite we can calculate reflection coefficient curves for both the E and the H-polarization, we are not able to obtain results for both of them at the same time in COMSOL graphic userface – neither can we do after exporting our model into the Matlab code and running the routine. Thus analysis has to be worked out in sequences with appropriate changes in code.

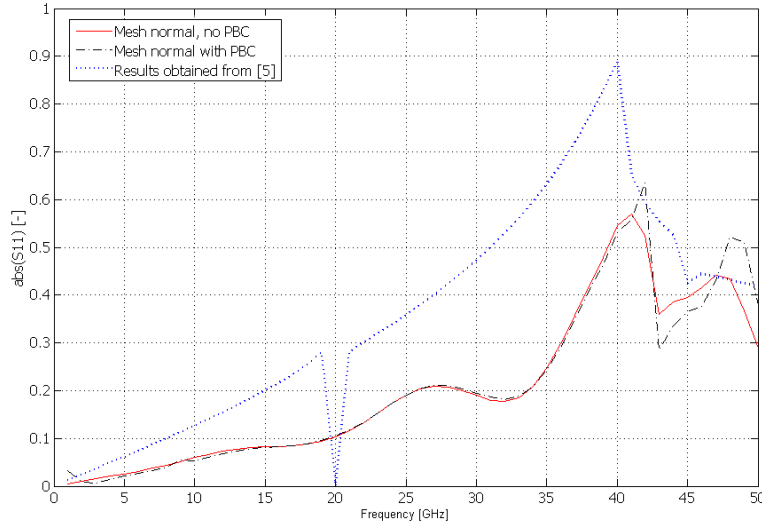


Fig. 5.4: The module of the reflection coefficient for the H-polarization.

5.10.1 Equivalent Feeding Modes

Although one H-polarization feeding port settings was already described, another working settings exists (settings with $E_{0y} = 0 \text{ Vm}^{-1}$ and *Eigenmode given by E field* should be changed to $E_{0x} = 0 \text{ Vm}^{-1}$ and *Eigenmode given by H field*). Both options are equal and it is only on a designer's best wish which one to use.

5.11 Adding Periodic Boundary Conditions

From all the settings made so far, adding periodic boundary conditions is the most exhausting one. To make them run in 3D, there is a variable implementing an extra equation to explicitly set the divergence of the D or B field to zero. This variable Ψ must also be made periodic [3]. Moreover, vector elements for the electric and magnetic field are used. PBC settings for the E and the H-polarization are identical and applied from the back to the front wall and from the left to the right wall.

1. Choose *Properties* from the *Physics* menu and set the *Divergence condition* On.
2. Go to *Physics*>*Periodic Conditions*>*Periodic Boundary Conditions*.
3. In the *Source* tab, choose boundary 1 (left wall) from the *Boundary selection* list.
4. Type `psi` in the *Expression* field. Text in the *Constraint name* is always generated automatically.
5. Select the *Vector element constraint* check box and type `tEx tEy tEz` to the next free *Expression field* below.
6. In the *Source* tab, choose boundary 5 (back wall) from the *Boundary selection* list and do the same procedure as for the left wall.

7. In the *Destination* tab, choose `pconstr3` from the *Constraint name* list. Choose boundary 7, select the *Use selected boundaries as destination* check box and type `psi` in the *Expression* field.
8. Choose `pconstr4x pconstr4y pconstr4z`, then boundary 7, select the *Use selected boundaries as destination* check box and type `tEx tEy tEz` in the *Expression* field.
9. In the *Destination* tab, choose `pconstr1` from the *Constraint name* list. Choose boundary 2, select the *Use selected boundaries as destination* check box and type `psi` in the *Expression* field.
10. Choose `pconstr2x pconstr2y pconstr2z`, then boundary 2, select the *Use selected boundaries as destination* check box and type `tEx tEy tEz` in the *Expression* field.
11. Switch to the *Source Vertices* tab, select numbers 4, 2, 1 in the *Vertex selection* list and move them to the *Source vertices* list.
12. Switch to the *Destination Vertices* tab, select numbers 12, 10, 9 in the *Vertex selection* list and move them to the *Destination vertices* list.
13. Choose another constraint in the *Constraint name* list and set *Source Vertices* and *Destination Vertices* for remaining constraints according to the Tab. 5.5. Always remember to select numbers of vertices in order as stated in the this table.
14. Click *OK*.

Tab. 5.5: Source and destination vertices numbers used for PBC.

Constraint name	Source Vertices	Destination Vertices
<code>pconstr1</code>	4, 2, 1	12, 10, 9
<code>pconstr2x pconstr2y pconstr2z</code>	4, 2, 1	12, 10, 9
<code>pconstr3</code>	4, 12, 11	2, 10, 9
<code>pconstr4x pconstr4y pconstr4z</code>	4, 12, 11	2, 10, 9

6 SETTINGS CASE STUDY

6.1 A Comparison of Results Obtained with and without PBC

Results for the E-polarization (cases with and without PBC) and for the H-polarization (no PBC) have been so far more or less successfully compared to curves obtained in [5]. An attentive reader might have a question whether it is necessary to use PBC.

As usual in the technical practice, we are looking for some kind of trade off, while assuming a sufficiently small frequency step and a correct placing of the feeding boundary. It should be stated in the first place, that it is rather hard to decide which curve of the no-PBC – PBC pair is more correct (see Fig. 5.3 again). They are both close to the ideal solution, appearing with the perfect match from zero up to frequency around 20 GHz and with markable differences in the range from 35 GHz to 50 GHz. Their nonsimilarity and a possible calculation error (if there is some) in this upper range can have two origins:

- In the no-PBC case, the assumption of an infinitely large plane is not fulfilled.
- In the PBC case, the mesh density (especially on boundaries at which PBC are applied) is not sufficient and errors are cumulated while the structure is being spread to the infinity in extent.

While a computational power of commonly available desktop machines used for technical calculations is still limited, time issues going hand in hand with a mesh density and a frequency step (all curves in the thesis were calculated with 1 GHz step) come in mind. Thus contents of Tab. 6.1 and Tab. 6.2 for the feeding edge position $\lambda/2$ and normal mesh should be compared. Interactive mesh procedure is driven by the minimum element quality parameter value (0.3410 depicts a normal mesh) and since the structures for both cases have the same dimensions, the same number of vertex, edge and boundary elements is used. The only and most unpleasant difference is a solution time, which is doubled for the PBC case (also holds for a fine mesh). All calculations and time measurements were made running Matlab code with Matlab connected to COMSOL Multiphysics.

Tab. 6.1: The feeding edge position, mesh density and a calculation time for the E-polarization without using PBC.

Feeding Edge Position	Mesh	Solution Time [s]	Number of Elements	Minimum Element Quality	DOF	N. of Vertex Elements	N. of Edge Elements	N. of Boundary Elements
$\lambda/4$	normal	193	5853	0.4066	7697	12	106	1168
$\lambda/2$	normal	150	5024	0.3410	6708	12	102	1128
$\lambda/2$	fine	452	9508	0.4061	12358	12	130	1684
$\lambda/2$	finer	4209	29324	0.3655	36789	12	184	3428
λ	fine	69	2555	0.4332	3594	12	98	798
λ	finer	197	197	0.3878	9753	12	130	1652

Tab. 6.2: The feeding edge position, mesh density and a calculation time for the E-polarization with PBC.

Feeding Edge Position	Mesh	Solution Time [s]	Number of Elements	Minimum Element Quality	DOF	N. of Vertex Elements	N. of Edge Elements	N. of Boundary Elements
$\lambda/2$	normal	295	5024	0.3410	7841	12	102	1128
$\lambda/2$	fine	1000	9508	0.4061	14383	12	130	1684

Since dimensions for the H-polarization modification have not changed, there will be no surprise while looking through the Tab. 6.3 and Tab. 6.4. Again, time needed while using PBC is doubled comparing the PBC and no-PBC case. Some deviations in the solution time can be considered minor and will be caused mostly by allocating the operating memory and a computational power of the CPU for programs running on the background. Also, time needed to reach the E and H-polarization

Tab. 6.3: The feeding edge position, mesh density and a calculation time for the H-polarization without using PBC.

Feeding Edge Position	Mesh	Solution Time [s]	Number of Elements	Minimum Element Quality	DOF	N. of Vertex Elements	N. of Edge Elements	N. of Boundary Elements
$\lambda/2$	normal	134	5024	0.3410	6708	12	102	1128
$\lambda/2$	fine	430	9508	0.4061	12358	12	130	1684

curves is comparable. One might want to discuss the influence of the mesh density

Tab. 6.4: The feeding edge position, mesh density and a calculation time for the H-polarization without using PBC.

Feeding Edge Position	Mesh	Solution Time [s]	Number of Elements	Minimum Element Quality	DOF	N. of Vertex Elements	N. of Edge Elements	N. of Boundary Elements
$\lambda/2$	normal	272	5024	0.3410	7841	12	102	1128
$\lambda/2$	fine	1120	9508	0.4061	14383	12	130	1684

to the accuracy of results. As can be seen from Fig. 6.1 showing reflection coefficient curves for two mesh densities with PBC used, shifting the mesh density one level up from the normal to the fine is followed by a slight curve's shape improvement and loaded by a huge solution time gap in a PBC case disadvantage (check Tab. 6.2).

6.2 Feeding Boundary Position Analysis

The feeding boundary position placed in a $\lambda/2$ distance in front of the conductive patch was stated and recommended without giving any explanation. Unfortunately, there is no math helping us to find a correct placing of this boundary for various frequency ranges. Thus its position has to be found out empirically running through calculations, while moving the boundary closer and further. Two utmost distances

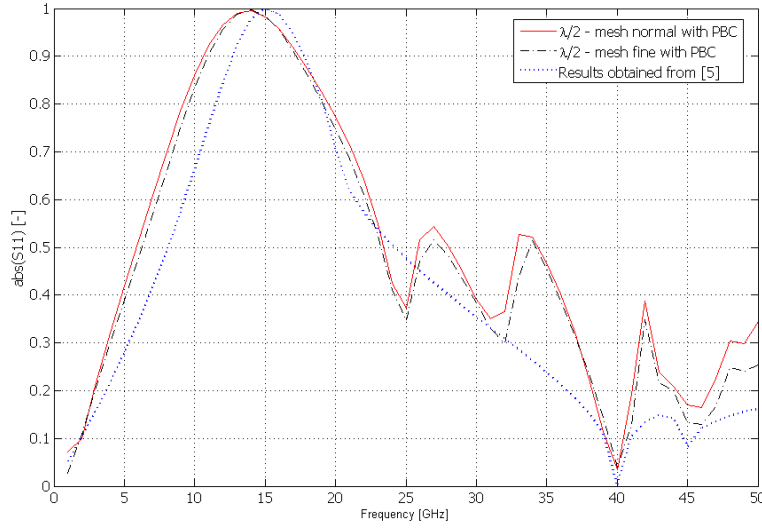


Fig. 6.1: The module of the reflection coefficient for the E-polarization with different mesh densities and PBC used.

exist, though. The closest distance should not be less than the wavelength of the lowest frequency in the analyzed frequency range and the most distant position should be kept as small as possible to use as little mesh elements as we can. Feeding edge movement beyond this distance does not harm the model's functionality and can be recommended in cases we do not care too much about the mesh elements number.

Curves for different feeding boundary positions are plotted in Fig. 6.2. The optimal distance found was $\lambda/2$, where λ is a wavelength at frequency 15 GHz. Nevertheless, remember to move the feeding boundary as far as you can if you have enough computational capacity.

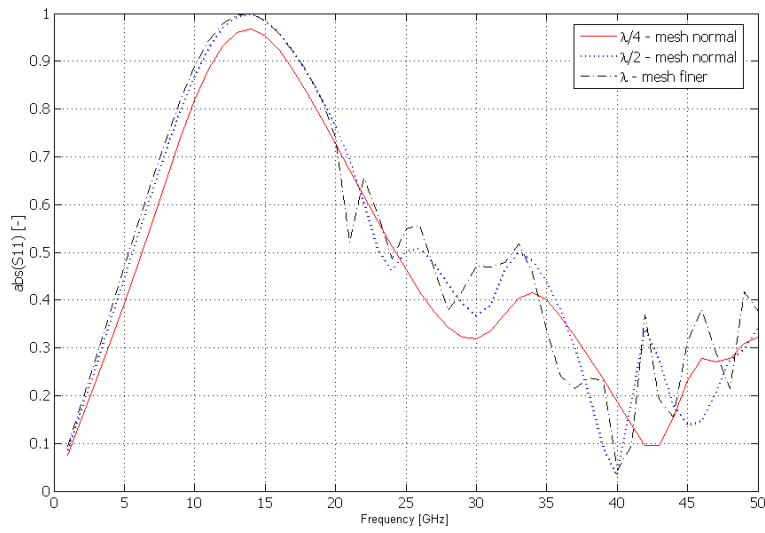


Fig. 6.2: The feeding boundary position for the E-polarization (works for the H-polarization as well).

7 OCCUPIED ELEMENTS

We have so far analyzed a simple patch element placed in the middle of the air box, where the air box around the patch defined the gap between the elements. This arrangement can be redrawn into a formation with four identical rectangles placed in the corners (see Fig. 7.1) with no expected changes in reflection coefficient curves.

From the modeling point of view, there is a new situation we have to be aware of. The patch or any other shape is not placed in the middle and its metallic surface can touch or even cross boundaries of the air box. Calculations on a redrawn formation with four rectangles in the corners to test whether the arrangement with metallic objects intersecting the dimensions of the air box will lead to our model's failure are covered in this chapter.

Moreover, if our model works even for this arrangement, then it can be exploited to solve arrangements with more closely packed elements. Munk [2] calls this move of approaching of single elements closer as occupying. Note that occupying is used to shape reflection coefficient curves (the resonance and the bandwidth).

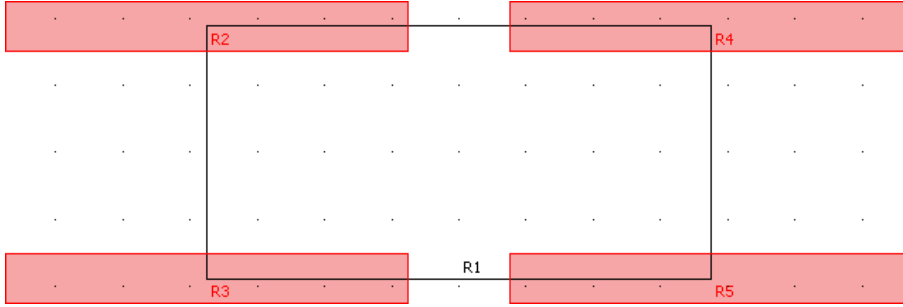


Fig. 7.1: A view from above at rectangular patches placed in the corners and crossing the borders of the air box. Four patch elements with dimensions $a = 12 \cdot 10^{-3}$ and $b = 1.5 \cdot 10^{-3}$ (a well known rectangular patch element from previous chapters) is placed in a manner that their inter element spacing is the same as for the element placed in the middle of the air box.

Turning our attention back to Fig. 7.1, an object to analyze consists of an air box R1 (created in a new *Geom2* at the work plane set to $(x, y), z = 0$) with dimensions $A = 15 \cdot 10^{-3}$, $B = 7.5 \cdot 10^{-3}$. The air box is then extruded into a 3D with a $\lambda/2$ height. Four patches R2, R3, R4, R5 are drawn (again in a *Geom2* at the work plane set to $(x, y), z = 0$) by specifying its dimensions and positions of their centers.

Although on the position of the patches outside the air box wouldn't matter, they sort of don't look good and their presence increase the number of mesh points. To get rid of them, select the *Geom2* tab, then choose *Draw > Create Composite Object* from the main menu and type $R1 \cdot R2 + R1 \cdot R3 + R1 \cdot R4 + R1 \cdot R5$ into the *Set formula* field. Operators \cdot and $+$ sign intersection and union of geometric objects. The last step to take is to choose objects remaining after the joining operation and embed them into a 3D at the work plane level $(x, y), z = 0$. The final structure should appear as the one in Fig. 7.2. Since the redrawn geometry was on purpose created to reach the same reflection curves as the original middle placed rectangular patch, calculations were run to prove the design working. The model settings were

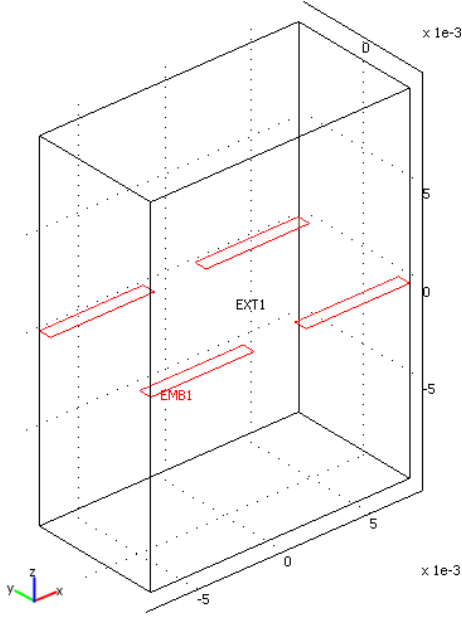


Fig. 7.2: The final occupied structure with conductive patches placed in corners.

the same as the one described within sections 5.3 – 5.9 (section Geometry Modeling is substituted by the description from the paragraph above), plus all four added conductive pathes touching the corners have to be set to PEC. Moreover, the H-polarization settings modification and equivalent feeding modes work without any changes needed. For the PBC case, only source and destination vertices has to be changed according to Tab. 7.1. Always remember to check twice whether the *Divergence condition* in *Physics>Properties* is set On, otherwise you're never gonna get the curve you expected. Back to obtained curves which can be seen in Fig. 7.3.

Tab. 7.1: Source and destination vertices numbers used for the redrawn structure with PBC.

Constraint name	Source Vertices	Destination Vertices
pconstr1	8, 24, 22	2, 19, 17
pconstr2x pconstr2y pconstr2z	8, 24, 22	2, 19, 17
pconstr3	8, 3, 1	24, 19, 17
pconstr4x pconstr4y pconstr4z	8, 3, 1	24, 19, 17

As understandable at the first sight, curves for the middle placed rectangular patch and for the redrawn structure (both without using PBC) are identical. As a little less pleasant, especially at frequencies under 15 GHz, comes out a comparison between one of these curves and the curve for an redrawn structure with PBC used. Reflection coefficient doesn't reach its maximum value, while the first resonant frequency is now at its ideal position according to [5] though. Also, a huge contrast in values is to be found from frequency 1 GHz to 7 GHz and continues up to 15 GHz. An origin of dissimilarity of the curves is unknown, but based on mesh density tests, the mesh density is not the factor to put the blame on.

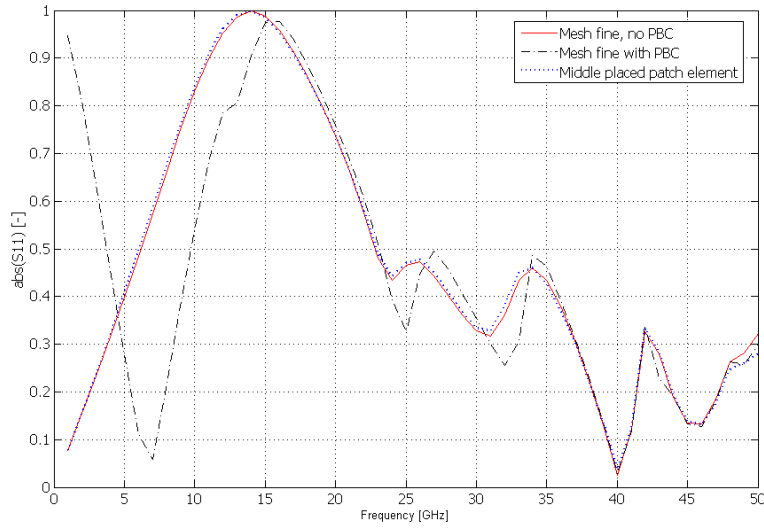


Fig. 7.3: The E-polarization reflection curves for the redrawn structure with (solution time 752 s) and without PBC (351 s) plotted against the middle placed patch reflection curve.

8 REAL PERIODIC STRUCTURES

It is not uncommon that periodic surfaces are first designed as free-standing and then (due to mechanical reasons, since the surface simply has to be placed on something) other layers (dielectrics) are added hoping the original design won't change much [2]. As will be shown within the content of this chapter, this idea is fundamentally wrong. Every added layer has a profound influence on the reflection curve. Namely, it forms the shape of the curve and what is of more importance, it causes resonant frequency shifts in direction downwards.

There are basically three cases arising from Maxwell's equations [2]. First, if a periodic surface had been covered from both sides by an infinite dielectric material of an infinite extent (with assumed ϵ_r), the resonant frequency reduction would reach its maximum with a factor $\sqrt{\epsilon_r}$.

Second, if the thickness of the dielectrics was reduced to a small thickness $d \sim 0.05\lambda_\epsilon$ at each side of the periodic structure, the resonant frequency will change to somewhere between f_0 and $f_0/\sqrt{\epsilon_r}$. Note, that even for thicknesses as small as $d \sim 0.05\lambda_\epsilon$, the resonant frequency is fairly close to $f_0/\sqrt{\epsilon_r}$.

Third, if we have a dielectric layer only to the one side of the periodic structure, the largest frequency reduction would be $f_0/\sqrt{\epsilon_r}$.

The behaviour described in recent three paragraphs is the same for dipole and slot periodic surfaces covered by dielectrics of a small thickness. However, if the layer(s) become thicker, more than $\lambda_\epsilon/4$, the two types will act differently [2].

8.1 Model of a Real Periodic Structure

A model with thin dielectric layers to the one and to the both sides of the periodic structure (Fig. 8.3) was created to confirm whether the COMSOL is able to offer correct results for such structures. An object to study is a chronically known middle placed rectangular patch with dimensions according to Tab. 5.3. What is new, are two thin layers to the both sides of the periodic structure with $\epsilon_r = 4$. Each extruded layer has a thickness $d = 0.5$ mm. The feeding boundary is now placed $\lambda/2$ from the upper boundary of the upper dielectric layer. The distance from the feeding boundary to the conductive patch is $\lambda/2 + d$ and the height of the whole bounding air box is $2 \cdot (\lambda/2 + d)$.

The model is set up in an usual manner. The Application Scalar Variables settings, Mesh, the Parametric analysis setup, the Postprocessing setup are the notorious ones used for a middle placed patch element without PBC. Adjustments have to be applied on boundary settings, where the back and the front wall remaining set as PMC, the left and the right are still PEC, the conductive patch is also PEC, the top boundary is Port, the bottom boundary is a non-reflecting Scattering boundary.

But, since we added dielectric layers, two new subdomains appeared. To decrease a number of mesh points and prevent overlapping of volumes, a composite object (operation *Union*) from the main menu *Draw > Create Composite Object* with the *Keep interior boundaries* check box selected should be created. This operation will result in a three new boundary planes and four subdomains in total. A relative

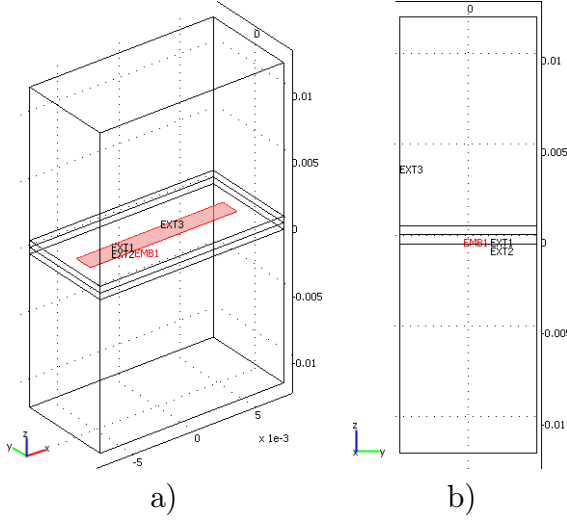


Fig. 8.1: A model of a real structure: a) 3D view on a structure with two thin dielectric layers with $d = 0.5$ mm and $\epsilon_r = 4$, b) the same model from a lateral view.

isotropic permittivity value $\epsilon_r = 4$ should be assigned to subdomains representing dielectric layers from the main menu *Physics > Subdomain Settings*. A Continuity boundary condition has to be assigned to the new trio of boundary conditions to force the continuity of the electric and magnetic field. Curves to prove the truth are not plotted in the thesis, but it was overviewed and positively tested, that Continuity boundary condition doesn't cause reflections and thereby have a zero impact on the shape of curves.

8.2 Dielectric Thickness

As you might spotted, a threshold thickness of a dielectric layer was defined as $d \sim 0.05\lambda_\epsilon$, so to the wavelength in dielectrics with relative permittivity ϵ_r . As we know from the FSS theory [2], a solid interior element should have a first resonance at the double of its biggest length, what sets us around 12.5 GHz. But to stay consistent and allow a conclusive comparison with results obtained so far, the first resonant frequency is chosen to $f_0 = 15$ GHz. The wavelength in dielectrics is then evaluated as $\lambda_\epsilon = c/(f_0\sqrt{\epsilon_r}) = 3 \cdot 10^8/(15 \cdot 10^9\sqrt{4})$. Finally, a threshold dielectric thickness $d \sim 0.05\lambda_\epsilon = 0.05 \cdot 0.01 = 0.0005$ m = 0.5 mm.

8.3 Results Comparison With Theory

Reflection curves are plotted in Fig. 8.2 and corresponding numeric data are presented in Tab. 8.1.

A wise move is to begin a comparison with a small dielectric thickness placed just over the periodic structure, such as $d = 0.25$ mm. A theoretical first resonant frequency reduction is maximally to 9.5 GHz. Our curve doesn't reach this value, what it is perfectly OK, since the shift is a matter of the thickness and there is no

formula to use to predict the exact value. Moreover, curve's shape is similar to the one of the free-standing structure, except the higher resonances are now at 34 GHz and 43 GHz.

Getting the model more complicated, a layer with $d = 0.25$ mm is added under the periodic structure. Due to a larger total distance which the wave has to propagate through, the first resonance is now even at a lower frequency (11 GHz), which again satisfies the condition in Tab. 8.1.

The last shot is at a layer placed over and under the structure, each with $d = 1$ mm and simulating the infinite thickness, since it satisfies condition $d > 0.05\lambda_e$. The first resonant frequency should be appearing close to 7.5 GHz (the lowest frequency from all curves). As seen from Fig. 8.2, curve's top is very close to this value. The only reason curve doesn't hit with its maximum a theoretical value is that the dielectric is not of an sufficient thickness, but still, its $d = 1$ mm is big enough to push the resonance almost at the lowest possible level.

About meshing, after inspecting Tab. 8.1, one might think that adding a thin dielectrics can't cause such an accrual of mesh elements, since the total structure's dimensions didn't changed so rapidly. This idea is completely true. The increase of a number of mesh elements exists because it is an automatic meshing procedure, working to reach the Minimal element quality value, we use. For thin subdomains, many small elements have to be used to reach the Minimal element quality value, while less elements are needed for thick subdomains (check Tab. 8.1 and a mesh element number for $d = 1$ mm and $d = 0.25$ mm and remember that for a thinner subdomain, even a one level less dense mesh was used to keep the number of elements at the acceptable number).

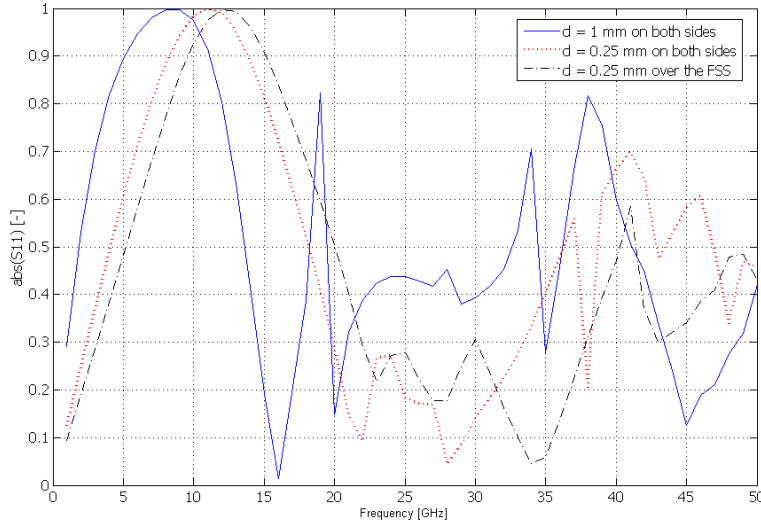


Fig. 8.2: E-polarization reflection curves for variable dielectric thicknesses d with $\epsilon_r = 4$ for feeding edge position $\lambda/2 + d$ from the conductive patch.

Tab. 8.1: A solution time table with expected new first resonant frequency values for various thicknesses of dielectrics with isotropic relative permittivity $\epsilon_r = 4$ placed on both sides of the structure (b) or just over the structure (o). The feeding boundary position $\lambda/2 + d$. The original first resonant frequency $f_0 = 15$ GHz.

d [mm]	Mesh	Number of Elements	DOF	Solution time [s]	New expected first resonant frequency
1 (b)	fine	7881	10331	fine	close to $f_0/\sqrt{\epsilon_r}$ (7.5 GHz)
0.25 (b)	normal	15311	19220	normal	between f_0 and $f_0/\sqrt{\epsilon_r}$ (15 GHz – 7.5 GHz)
0.25 (o)	normal	15311	19220	normal	max. $f_0/\sqrt{(\epsilon_r + 1)/2}$ (9.5 GHz)

8.4 Circular Ring Element Analysis

Free-standing rectangular patch element analysis results were described in previous chapters. This element is considered to be one of the simple ones. There is basically an unlimited number of available shapes sorted into four basic categories though, from which complicated shapes are derived [2]. Also as mentioned in [2], shape's symmetry is advantageous, since such an element acts the same for all scan angles within a chosen polarization. Therefore, a symmetric free-standing circular ring element belonging to the "Loops Type" group [2] with dimensions published in [4] was analyzed and compared to curves published in this source.

The circular ring element analysis settings is no different to the analysis of the rectangular patch element described from Chapter 5.3 to Chapter 5.11, clearly except the section Geometry Modeling. The dielectrics settings is done using the principle described in Chapter 8. Loop type elements are supposed to resonate, when their

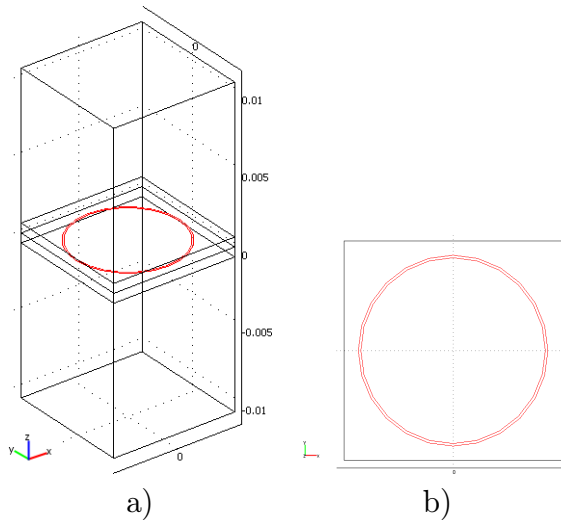


Fig. 8.3: A circular ring element model: a) a 3D view on the structure with two thin dielectric layers, each with $d = 0.064$ cm and $\epsilon_r = 3.5$, the square lattice spacing [4], the outer ring diameter 0.74 cm, the inner ring diameter 0.72 cm, the air box side length 0.85 cm, b) the same model from above.

average circumference is approximately one wavelength long [2], so considering the middle radius 0.73 cm, the resonance should appear somewhere around 13 GHz. Also, dielectric layers pull the frequency down. Unfortunately, result in [4] is plotted

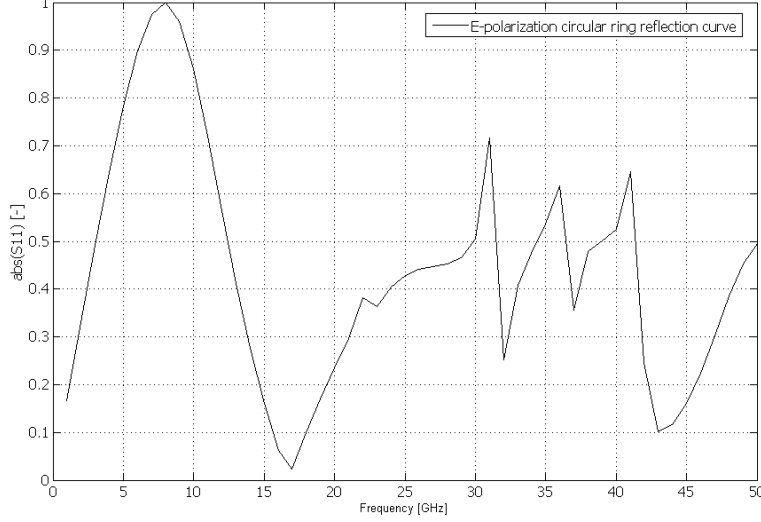


Fig. 8.4: The E-polarization reflection curve for a circular ring element. Number of mesh elements 13880, mesh normal, solution time 641 s.

for a transmission loss, thereby it can't be placed on a background of the comparing figure. Nevertheless, it can be seen (see Fig. 8.5) that maximum loss is at 8.4 GHz while our model (see Fig. 8.4) proves highest reflection at 8 GHz.

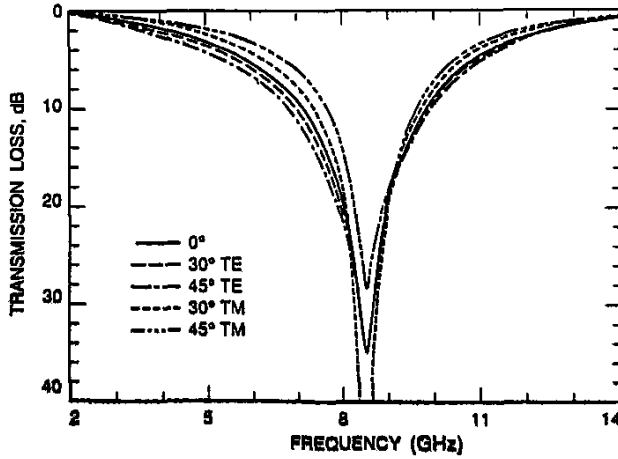


Fig. 8.5: The transmission loss for a circular ring element published in [4]. Two thin dielectric layers, each with $d = 0.064$ cm and $\epsilon_r = 3.5$, the square lattice spacing [4], the outer ring diameter 0.74 cm, the inner ring diameter 0.72 cm,

9 GLOBAL OPTIMIZATION ALGORITHM

Practical steps needed to execute the FSS analysis for various shapes were revealed and discussed in previous chapters. A designer is often facing a problem of finding the element's shape so its reflection coefficient (after expanding the element in extent to infinity) meets some previously chosen requirements, mostly described using a reflection coefficient curve as a function of frequency. Therefore it would be highly time saving to have a powerful numerical tool, which will be adjusting element's dimensions in a smart and automatic way to reach such a goal. A global optimization algorithm known as a Particle Swarm Optimization (PSO) will be applied on a free-standing rectangular patch without any dielectric layers and with the E-polarization of the incident wave.

9.1 Generating m-files

The main reason why COMSOL Multiphysics is so used and favoured is that it provides a connection to Matlab via a client-server communication. And a connection to Matlab means a well documented and fast calculation tool.

First, run COMSOL with Matlab otherwise you won't be able to treat data calculated by COMSOL in Matlab. The second step to make our design ready for an optimization is to draw and setup a model using the COMSOL user interface according to procedures published from Chapter 5.3 to Chapter 5.9.

Here comes the time to pay the highest attention. It is of the most importance to proceed just those described steps (open proper windows just once, click on the selected parts of the design just once). The model settings doesn't fall apart if you proceed those steps in a different order or open the settings windows twice, but you are going to pay the highest price – calculation time. Be aware everytime you change something (or even click on the structure) in the model, new lines of a Matlab code are generated and added to the end of the already existing code. Finally, you may wind up with thousands of lines instead of finishing with a few lines for our simple structure.

The conversion of a model from COMSOL Multiphysics to a Matlab code is done from the main menu *File>Save As* and by selecting *Model M-file (*.m)* in the *Files of type* listbox. The raw code is then ready to be opened in Matlab.

Adding a header, so the model can be called as a function, is a must for the purposes of the optimization. Check this header in the Appendix A, where dimensions for the conductive element are depicted as a, b and dimensions for the surrounding air box are depicted with A, B . The code also allows to choose the feeding edge position and a one of the total amount of ten mesh densities. The height of the air box is the doubled feeding edge position. The optimal feeding edge position is $\lambda/2$ at the frequency 15 GHz. Two terms (the first for a boundary settings and the second for the feeding with an incident wave) have to be modified to make the model calculate the reflection coefficient for the H-polarization case.

An access to data deserves a special attention. The solution data are stored within a data structure, which is accessed via a COMSOL Script function

`posteval(xfem,'abs(S11_rfw)','Edim',0,'Solnum','all')` belonging to a Postprocessing Functions group. This function is presented to evaluate expressions in subdomains, boundaries, edges or vertices [3]. The expression to evaluate is `'abs(S11_rfw)'` – the module of the reflection coefficient. The value 0 attached to the `'Edim'` parameter defines, that only values from vertices want to be pulled out (`'Edim'` value 1 would pull out the data from edges, 2 then from boundaries and finally 3 from subdomains). The value `'All'` attached to the `'Solnum'` parameter causes that data are pulled out for all 12 vertices appearing in our structure.

Although converting the model to a Matlab code allows a simple postprocessing of the data, a new model and m-file have to be created for different structures placed within the air box (the boundary and feeding settings stay unchanged comparing to the rectangular patch element). Using the COMSOL graphic interface is by far the easiest option to draw and setup the model. Of course objects can be created using COMSOL Script, but this approach is complicated and predisposed to make code errors.

9.2 Particle Swarm Optimization

The PSO is a robust stochastic evolutionary computation technique based on the movement and intelligence of individuals (also known as particles or agents). It has been shown that PSO outperforms other methods (genetic algorithms) of optimization in certain instances [6].

The whole principle is usually described using a swarm of bees in a field. The goal of the principle is to find in the field the location with the highest density of flowers without any knowledge of the field a priori. The bees start looking in random locations with random velocities, but never exceeding the maximum allowed velocity in a given direction. During their movement, every bee can remember the location where it found most flowers (personal best) and also somehow knows other locations where the other bees found its personal bests. As the bees fly and explore the field with kind of movement fully described in [6], they are overflying locations of greatest concentration and are pulled back toward them. Also, bees are overflying previously encountered locations of highest concentration hoping to find the absolute highest concentration of flowers (global best).

Moreover, every bee in the swarm appears at some place in the field (*position*). This position is generally somewhere in a N-dimensional *solution space* chosen according to the problem. All evolutionary computation techniques require some function or method to evaluate the goodness of a position. The fitness function must take the position in the solution space and return a single number representing the value of that position (this would be the density of flowers in analogy with our demonstrating case). The fitness function represents the link between the optimization and the physical problem and could in general be antenna gain, weight or some kind of weighted sums of those factors [6].

Three types of boundary conditions are imposed by authors of [6] to keep search to what is physically possible. When being hit, *Absorbing Walls* zero the particle's velocity, but allows the particle to be pulled back to the allowed solution space.

Reflecting Walls change the sign of the velocity of the particle when being hit. Particle then continues exploring in the allowed solution space.

Invisible Walls define the solution space (locations where fitness will and will not be evaluated).

The core element of the whole method is an adjustment of particle's velocity, which is changed according to relative locations of personal and local bests. The particle's velocity is regularly updated with a time-step Δt . Most literature omits this value, therefore assuming its value to be one. Source [6] refers that value Δt can be factored out of equations describing the relation between the values of c_1 , c_2 and ω . Thus value of Δt is implied in the selection of the other parameters. Note that value c_1 is a factor determining how much the particle is influenced by the memory of his best location (increasing c_1 encourages exploration of the solution space) and c_2 is a factor determining how much the particle is influenced by the rest of the swarm (increasing c_2 encourages exploitation of the supposed global maximum). ω , known as inertial weight, is chosen to be between 0.0 and 1.0 and determines to what extent the particle remains along its original course unaffected by the pull of global and local best.

9.2.1 Code for the PSO

The complete PSO Matlab code for a middle placed rectangular patch element can be seen in Appendix B. The input of the main function is formed by two numbers. I defines how many individuals will be used within one generation and G defines a number of generations. Each generation differs from the previous one by a change of dimensions controlled by the PSO. The objective function (an optimal case to which we want our solution to be close as possible) is a reflective coefficient curve obtained with [5] for dimensions $a = 12$ mm, $b = 1.5$ mm, $A = 15$ mm, $b = 7.5$ mm.

The mesh density set to level normal, minimal frequency, maximal frequency and a number of equidistantly placed steps within such defined frequency range are declared as constants, since they are seldom changed (although they can be quickly placed in the function's definition if needed). Also, the objective function is loaded in the same section.

Individuals' dimensions in the first generation are taken from a random guess (see lines 25-28 in Appendix B). The guess is highly dependent on the constants used on those lines. The further you set the constants away from the expected solution dimensions, the more generations you are going to need to reach your goal. Lines 29-30 are present just to keep dimensions of the conductive patch smaller than dimensions of the surrounding air box.

The selection of the best individual (evaluating fitness) is based on counting squares of the differences measured from the reflection coefficient curve to the objective function (see line 44 in Appendix B). The fitness values are listed in the Matlab prompt along with dimensions for each individual. The individual with the lowest error related to the objective function is chosen after completing the solutions for all individuals in the actual generation (line 48 in Appendix B).

The last crucial step is to adjust model's dimensions and agent velocities between single generations (lines 58-60). Both are influenced by constants defined on lines 18-

19 (set to values recommended by [6]). Modification of these scaling factors doesn't influence the optimization as much as the value of time-step dt does. Change the value of dt to 0.01 or 0.1 four rough estimates.

9.3 Results

PSO was let to work for a different number of individuals within one generation and for a varying number of generations (remember to use a function `format long` to increase a number of displayed digits in the Matlab prompt, because the implicit number of displayed digits may not be sufficient to spot small differences between dimensions). Dimensions and the fitness for some typical algorithm runs are listed in Tab. 9.1. An amount of generations not lower than three and a number of

Tab. 9.1: PSO results for a varying number of generations G and individuals I within one generation.

(G, I)	a [m]	b [m]	A [m]	B [m]	Solution time [s]	Fitness
(2,4)	0.01234	0.00155	0.01412	0.00764	1265	0.7527
(3,6)	0.01112	0.00143	0.01574	0.00738	2856	0.4016
(2,9)	0.01252	0.00165	0.01501	0.00793	2768	1.0044
(4,5)	0.01161	0.00169	0.01468	0.00740	3211	0.7749
(1,10)	0.00114	0.00140	0.01428	0.00745	1458	0.6809
(3,9)	0.00113	0.00170	0.01587	0.00791	4364	0.4307

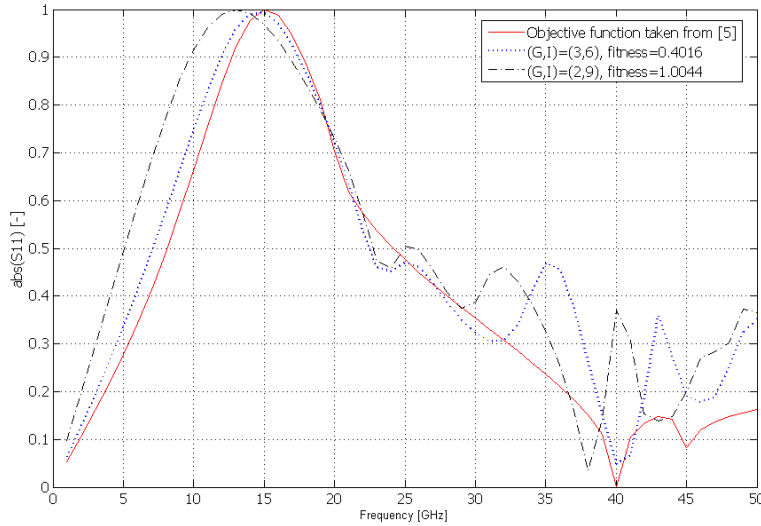


Fig. 9.1: Resulting reflection coefficient curves after several PSO runs and various numbers of generations (G) and individuals (I). Runs with a number of generations equal to three offered the best results.

individuals in a single generation around nine should be used according to results in Tab. 9.1. An often stated value of eight generations and eight individuals can be

used, but will proportionally extend the calculation time. Using a high number of individuals and just one generation is controversial. The random guess procedure generates the set of slightly different dimensions and we can hit the best fitness value at the first shot if we are lucky enough. On the other hand, the algorithm will not have a chance to modify dimensions since there are no other generations to be calculated. Therefore a number of generations higher than one is advised to allow the modification of dimensions according to the velocity of the individuals, the inertial weighting factor and others (see line one in Tab. 9.1 with a perfect fitness result). Also note that a good optimization result is not guaranteed even when using a high number of individuals and generations (see Tab. 9.1, line three). This is caused by a dependence on the initial guess, which wasn't too good this time. Hence the algorithm should be run through a couple of times to find the best result.

The calculation time can be predicted having the experience from analysis mentioned early in this thesis. A solution period for one individual should take around 150 s for a case with no-PBC used. Hence a total solution time for two generations and eight individuals within one generation will result in a time period approximately $16 \cdot 150 = 2400$ s. This assumption unfortunately holds only in a limited manner (when dimensions of the rectangular patch are not too close to dimensions of the air box). If you or the PSO algorithm for some reason change the dimensions of the two mentioned above too close, the automatic meshing procedure will do the meshing to reach a given minimum element quality value. In other words, it will use many small elements to mesh these small areas. Since large areas may still exist and the growth of the elements is on purpose limited (a given minimum element quality value must be achieved on the whole design), the polygons grow slowly and many small elements (smaller than actually needed) are used. You encounter this kind of behaviour always when meshing objects with mutually non proportional dimensions. A shot how to escape out of this would be to use a manually set meshing procedure – to set a minimal element size for each subdomain, set growing of elements and so on. This can be easily done via COMSOL Graphic interface and not that easily through COMSOL Script. Moreover, the code to control whether the number of elements used to mesh the whole structure isn't too high or too low would be needed.

10 CONCLUSION

Basic research to prove modeling of FSS working was carried out on a 1 Dimensional FSS using a 2D In-Plane Waves Module. Two cases, the first with and the second without using periodic boundary conditions offered the same curves for the module of the reflection coefficient. Solution time differences between those cases were minor due to analyzing in 2D. The 2D In-Planes Module was not found sufficient to fully analyze FSS.

The 3D Electromagnetic Waves Module was used instead to allow analysis of FSS with periodicity in two dimensions. Primary calculations were focused on building the running model environment for a middle placed rectangular free-standing FSS – how to most effectively draw the structure, how to feed the structure, where put the feeding boundary and how to setup periodic boundary conditions. All issues were solved and showed some positives (availability to reduce the number of mesh elements using smart drawing techniques) and negatives (unwanted appending of the Matlab code) of the COMSOL Multiphysics graphic user interface.

A variable Ψ implementing an extra equation to explicitly set the divergence of the D or B field to zero and the vector element constraint tEx tEy tEz are necessary to run periodic boundary conditions. Unfortunately, solving those two extra equations introduces a massive increase of a solution time. The time period needed is doubled comparing to the no-PBC case with almost no difference in the shape for a module of the reflection coefficient. Curves calculated for a middle placed rectangular patch and the E and the H-polarization were very close to ones calculated with applet published in [5].

Adding thin dielectric layers (its thickness is determined to the wavelength in the medium) enabled a comparison of curves obtained with COMSOL Multiphysics to curves published in [2] and [4]. Various dielectric thicknesses and arrangements simulated three extreme cases. Layers did cause resonant frequency shifts as expected and results matched.

Global optimization algorithm PSO was introduced in the last chapter. The algorithm changes the dimensions of the rectangular patch and the surrounding air box so the reflection coefficient curve fits the objective function (reflection coefficient curve obtained with [5]). The match is not perfect though. There are in general two reasons to explain that. First, COMSOL Multiphysics calculates with some error comparing to results obtained with [5] (assuming the same dimensions). Second, Munk [2] says that curves for a chosen element type can be shaped only in a limited manner (e.g. by packing the elements) and therefore you can not expect to obtain arbitrary reflection coefficient curves. The latter reason is of a minor influence in this case.

Many other models and simulations in addition to ones published in this thesis were created during my work. One example for all, perfectly matched layer used under the bottom of the air box hoping to reduce reflections didn't lead to any increase of accuracy and slowed calculations (a subdomain was added).

Inability to compute S-parameters values using an analytical formula (port had to be used to generate the incident wave) weakened the potential of the model. This complication escalated in inability to analyze FSS for an arbitrary angle of incidence.

BIBLIOGRAPHY

- [1] RAIDA, Z. et al. Analýza mikrovlnných struktur v časové oblasti. Brno: Nakladatelství VUTIUM, 2004. ISBN 8-0214-2541-5
- [2] MUNK, B. A. Frequency Selective Surfaces: Theory and Design. New York: John Wiley and Sons, 2000. ISBN 0-4713-7047-9
- [3] COMSOL Multiphysics 3.3 User's Guide. Stockholm: COMSOL, 2007.
- [4] WU, T. K. Frequency Selective Surface and Grid Array, New York: John Wiley and Sons, 1995, ISBN 0-471-31189-8
- [5] RAIDA, Z.: a et al. Multimedia Textbook of EM Waves and Microwaves [online]. Brno. Brno University of Technology, Dept. of Radio Electronics. Available from WWW. http://www.urel.feec.vutbr.cz/~raida/multimedia_en/chapter-5/5.1E.html.en, cited on 4.3.2008
- [6] Robinson, J. and Rahmat-Samii, Y., Particle Swarm Optimization in Electromagnetics, IEEE Transactions on Antennas and Propagation, Vol. 52, No. 2, February 2004, pp. 397-407

SYMBOLS AND DEFINITIONS

FSS	Frequency Selective Surface
PBC	Periodic Boundary Conditions
FEM	Finite Element Method
PMC	Perfect Magnetic Conductor
PEC	Perfect Electric Conductor
PML	Pefectly Matched Layers
PSO	Particle Swarm Optimization
CBC	Continuity Boundary Condition
PDE	Parcial Differential Equation

APPENDIX

A	M-file of the model	57
B	PSO code	59

A M-FILE OF THE MODEL

```

01 function out = univ(a,b,A,B,mden,fmin,fmax,step)
02 %a - length of the conductive patch [m]
03 %b - width of the conductive patch [m]
04 %A - length of the airbox [m]
05 %B - width of the airbox [m]
06 %mden - mesh density (10, ..., 6-Coarse, 5-Normal, 4-Finer, ..., 1)
07 %fmin - min. frequency [Hz]
08 %fmax - max. frequency [Hz]
09 %step - number of lineary distributed steps within the frequency range
10
11 f = 15e9; c = 3e8; lam = c/f;      %lambda
12
13 %Choose the feeding edge position (related to the wavelength at 15GHz)
14 %lam = lam;      % lambda
15 lam = lam/2;      % lambda/2
16 %lam = lam/4;      % lambda/4
17
18 %%%%%%%%%%%%%%%%%%%%%%%%%%%%%%%%%%%%%%%%%%%%%%%%%%%%%%%%%%%%%%%%%%%%%%%%%
19 % COMSOL Multiphysics Model M-file
20 flclear xfem
21
22 % COMSOL version
23 clear vrsn
24 vrsn.name = 'COMSOL 3.3'; vrsn.ext = ''; vrsn.major = 0; vrsn.build = 405;
25 vrsn.rcs = '$Name: $'; vrsn.date = '$Date: 2006/08/31 18:03:47 $';
26 xfem.version = vrsn;
27
28 % Geometry 2
29 g1 = rect2(num2str(a),num2str(b),'base','center','pos',{ '0','0'},'rot','0');
30 g2 = rect2(num2str(A),num2str(B),'base','center','pos',{ '0','0'},'rot','0');
31 g3 = embed(g1,'Wrkpln',[0 1 0;0 0 1;0 0 0]);
32 g4 = extrude(g2,'distance',[2*lam],'scale',[1;1],'displ',[0;0],...
33     'twist',[0],'face','none','wrkpln',[0 lam 0; 0 0 lam; -lam -lam -lam]);
34
35 % Geometry 1
36 flclear fem
37
38 % Analyzed geometry
39 clear f s
40 f.objs = {g3}; f.name = {'EMB1'}; f.tags = {'g3'};
41 s.objs = {g4}; s.name = {'EXT1'}; s.tags = {'g4'};
42 fem.draw = struct('f',f,'s',s); fem.geom = geomcsg(fem);
43
44 % Initialize mesh for geometry 1
45 fem.mesh = meshinit(fem,'hauto',mden);
46 xfem.fem{1} = fem;
47
48 % Geometry 2
49 flclear fem
50
51 % Geometry objects
52 clear s; s.objs = {g1,g2}; s.name = {'R1','R2'}; s.tags = {'g1','g2'};
53
54 fem.draw = struct('s',s); xfem.fem{2} = fem;

```

```

55 fem = xfem.fem{1};
56
57 % Application mode 1
58 clear appl
59 appl.mode.class = 'ElectromagneticWaves'; appl.module = 'RF';
60 appl.gporder = 2; appl.cporder = 1; appl.border = 'on';
61 appl.assignsuffix = '_rfw';
62 clear bnd
63 bnd.inport = {0,0,0,1};
64 bnd.E0 = {{0;0;0},{0;0;0},{0;0;0},{1;0;0}}; %Last term for E-pol{0;1;0}
65 bnd.type = {'EO','HO','SC','port'};
66 bnd.scsources = {'E','E','I','E'};
67 bnd.ind = [1,2,3,4,2,1,1]; %E-pol [1,2,3,4,2,1,1], H-pol [2,1,3,4,1,1,2]
68 appl.bnd = bnd;
69 appl.var = {'nu','freq','EOix','0'};
70 fem.appl{1} = appl; fem.frame = {'ref'};
71 fem.border = 1;
72 clear units; units.basesystem = 'SI'; fem.units = units;
73 xfem.fem{1} = fem;
74
75 fem = xfem.fem{2};
76 fem.sdim = {'x','y'}; fem.border = 1; clear units; units.basesystem = 'SI';
77 fem.units = units;
78 xfem.fem{2} = fem;
79
80 % Multiphysics
81 xfem = multiphysics(xfem);
82
83 % Extend mesh
84 xfem.xmesh = meshextend(xfem,'geoms',[1]);
85
86 % Solve problem
87 xfem.sol = femstatic(xfem, ...
88                     'solcomp',{'tExEyEz10'}, ...
89                     'outcomp',{'tExEyEz10'}, ...
90                     'pname','freq', ...
91                     'plist',[linspace(fmin,fmax,step)], ...
92                     'oldcomp',{'','linsolver','spooles'});
93
94 % Save current fem structure for restart purposes
95 fem0 = xfem;
96
97 %Pull data out of the solution structure
98 bod = posteval(xfem,'abs(S11_rfw)','Edim',0,'Solnum','all');
99 out = bod.d(:,1);

```

B PSO CODE

```

01 function [out,tim] = main( G, I)
02 % G - number of generations (iteration cycles)
03 % I - number of individuals in each generation
04 % x(1)= a - length of the conductive patch [m]
05 % x(2)= b - width of the conductive patch [m]
06 % x(3)= A - length of the airbox [m]
07 % x(4)= B - width of the airbox [m]
08
09 mden = 5;                % set mesh density normal
10 fmin = 1e9;
11 fmax = 50e9;
12 step = 50;
13
14 t1 = clock;              % time start stamp
15 load E_pol.S.mat;       % objective function
16
17 dt = 0.001;              % time-step
18 c1 = 1.49;               % scaling factor (1.49)
19 c2 = 1.49;               % scaling factor (1.49)
20
21 x = zeros( I, 5);        % agent position
22 p = zeros( I, 5);        % personal best
23
24 for n=1:I                % initial guess and dimensions restrictions
25     x(n,1) = 11e-3 + 2e-3*rand(); p(n,1) = x(n,1);
26     x(n,2) = 1.3e-3 + 1e-3*rand(); p(n,2) = x(n,2);
27     x(n,3) = 14e-3 + 2e-3* rand(); p(n,3) = x(n,3);
28     x(n,4) = 7.0e-3 + 1e-3* rand(); p(n,4) = x(n,4);
29     if x(n,3) <= x(n,1), x(n,3) = x(n,1) + 0.002; end
30     if x(n,4) <= x(n,2), x(n,4) = x(n,2) + 0.002; end
31     p(n,5) = 1e+6;        %set max. error
32 end
33
34 v = rand( I, 4);         % agent velocity
35 g = zeros( 1, 4);        % global best
36 e = zeros( G+1, 1); e(1) = 1e+6;
37
38 for m=1:G                % +++ MAIN ITERATION LOOP +++
39
40     w = 0.5*(G-m)/G + 0.4; % inertial weight
41     %%%%%%%%%%%%%%%%%%%%%%%%%%%%%%%%%%%%%%%%%%%%%%%%%%%%%%%%%%%%%%%%%%%%%%%%%Solve Using Comsol Script%%%%%%%%%%%%%%%%%%%%%%%%%%%%%%%%%%%%%%%%%%%%%%%%%%%%%%%%%%%%%%%%%%%%%%%%
42     for n = 1:I
43         vekt = univ(x(n,1),x(n,2),x(n,3),x(n,4),mden,fmin,fmax,step);
44         res = sum((vekt-stpf).^2);
45         x( n, 5) = res
46     end
47
48     [e(m+1),ind] = min( x( :,5)); % the lowest error
49
50     if e(m+1)<e(m)
51         g = x( ind, 1:4); % the global best
52     end
53
54     for n=1:I

```

```

55     if x(n,5)<p(n,5)                                % the personal best
56         p(n,:) = x(n,:);
57     end
58     v(n,:) = w*v(n,:) + c1*rand()*( p(n,1:4)-x(n,1:4));
59     v(n,:) = v(n,:) + c2*rand()*( g(1,1:4)-x(n,1:4));
60     x(n,1:4) = x(n,1:4) + dt*v(n,:);
61     if x(n,1) > 14e-3, x(n,1)=14e-3; end % absorbing walls
62     if x(n,2) > 14e-3, x(n,2)=14e-3; end
63     if x(n,3) > 15e-3, x(n,3)=15e-3; end
64     if x(n,4) > 15e-3, x(n,4)=15e-3; end
65     if x(n,3) <= x(n,1), x(n,3) = x(n,1) + 0.002; end
66     if x(n,4) <= x(n,2), x(n,4) = x(n,2) + 0.002; end
67 end
68
69 end
70 plot( e);                                % plot the error function
71 out = g;
72
73 t2 = clock;                                % time stop stamp
74 tim = etime(t2,t1);

```